Approximate A-priori Estimation of the Response Amplification Due to Geometric and Young's Modulus Mistuning

by

Saurav Sahoo

A Thesis Presented in Partial Fulfillment
of the Requirements for the Degree
Master of Science

Approved December 2014 by the
Graduate Supervisory Committee:

Marc Mignolet, Chair
Aditi Chattopadhyay
Jay Oswald

ARIZONA STATE UNIVERSITY

May 2015

ABSTRACT

Monte Carlo simulations are traditionally carried out for the determination of the amplification of forced vibration response of turbomachine/jet engine blades to mistuning. However, this effort can be computationally time consuming even when using the various reduced order modeling techniques. Accordingly, some investigations in the past have focused on obtaining simple approximate estimates for this amplification. In particular, two of these have proposed the use of harmonic patterns of the blade properties around the disk as an approximate alternative to the many random patterns of Monte Carlo analyses. These investigations, while quite encouraging, have relied solely on single degree of freedom per sector models of the rotor.

In this light, the overall focus of the present effort is a revisit of harmonic mistuning of rotors focusing first the confirmation of the previously obtained findings with a more detailed model of the blisk in both conditions of an isolated blade-dominated resonance and of a veering between blade and disk dominated modes. The latter condition cannot be simulated by a single degree of freedom per sector model. Further, the analysis will consider the distinct cases of mistuning due to variations of material properties (Young’s modulus) and geometric properties (geometric mistuning). In the single degree of freedom model, both mistuning types are equivalent but they are not, as demonstrated here, in more realistic models. The difference arises because changes in geometry induce not only changes in natural frequencies of the blades alone but of their modes and the importance of these two sources of variability is discussed with both Monte Carlo simulation and harmonic mistuning results.

The present investigation focuses also on the possible extension of the harmonic mistuning concept and of its quantitative information that can be derived from such analyses. From it, a novel measure of blade-disk coupling is introduced and assessed in comparison with the coupling index introduced in the past. In conclusions, the low cost of harmonic mistuning computations in comparison with full Monte Carlo simulations is demonstrated to be worthwhile to elucidate the basic behavior of the mistuned rotor in a random setting.

ACKNOWLEDGMENTS

I would like to thank, first and foremost, my advisor Dr. Marc Mignolet for his patient guidance and continuous support throughout this project and my study at Arizona State University.

I would also like to thank Dr. Aditi Chattopadhyay and Dr. Jay Oswald, for their participation and willingness to serve as members of my graduate supervisory committee.

The invaluable collaboration and support of Dr. Xiaoquan Wang, and the encouragement and support of Dr. Raghavendra Murthy is greatly appreciated.

Thanks also go out to the ASU Advanced Computing Center (A2C2) who's Saguaro and Medusa computing clusters proved invaluable for the large number of simulations carried out in this work.

Finally, I would like to thank all my peers and friends for providing encouragement and support at all times.

TABLE OF CONTENTS

LIST OF FIGURES

Figure Page

Figure Page

Figure Page

Figure Page

CHAPTER 1

INTRODUCTION AND REVIEW

1.1 MISTUNING

Bladed disks are typically designed to exhibit rotational symmetry, i.e. a rotation of the system by an angle of $n\varphi$, where $\varphi = 2\pi/N, N$ being the number of blades, will leave the structural and geometric properties unchanged. Such bladed disks are referred to as *tuned* and their vibration response possesses a series of properties which are reminiscent of the circular disk [1]. First, their mode shapes can be characterized by a number of nodal diameters in that the corresponding displacements of points at the same distance from the center but at angles φ, 2φ,3φ etc. of each other are sampled from the curves $\sin p\theta$ and $\cos p\theta$ where θ is the angle of the point from a fixed reference. The frequency p in these curves is the number of nodal diameters. The natural frequencies corresponding to these mode shapes are repeated for all modes with $p \neq 0$ to allow the existence of both $\sin p\theta$ and $\cos p\theta$ mode shapes.

The rotational symmetry of each component of the engine/turbomachine (rotors, stators, fuel nozzles, etc.) suggests that the flow field will also exhibit similar harmonic components of the form $\sin r\theta$ and $\cos r\theta$, referred to as engine order excitations with r being the engine order (EO). Owing to the orthogonality of the $\sin p\theta$ and $\cos p\theta$ functions, an rth engine order excitation induces modal forces in only the $p = r$ nodal diameter modes leading to significant simplifications in the computations of the forced steady state response of the bladed disks. In fact, such a response can be derived from an appropriate analysis, finite element typically, of just a sector under appropriate periodicity conditions. Such analyses are referred to as cyclosymmetric or sector analyses.

Mistuning refers to blade to blade variations of their properties, either material (Density, Young's modulus, etc.) and/or their geometry. These variations, induced by the finite tolerances of the manufacturing process and/or in-service wear or damage, are typically small but their effects on the steady state response of the rotor are often much larger. Blade-to-blade variations of their natural frequencies by a few percent have been reported to generate changes, increases in particular, of the forced response of some blades by 50%, 100%, and even larger. These increased responses are expected, and have been found, to lead to significant reductions in fatigue life of the blades.

The existence of this severe sensitivity has equally important computational implications. Indeed, by its nature, mistuning perturbs the rotational symmetry of the bladed disk structure and thus prevents the use of cyclosymmetric/sector analyses thereby leading to a large increase in the computational cost of a vibration analysis. Moreover, given their origin, the exact variations of the blade properties are typically not known in advance and vary from one physical bladed disk to another. Accordingly, the most appropriate representation of these properties is in terms of random variables recasting the prediction of the response as a random vibration problem. Unfortunately, no closed form solution for the statistics, e.g., mean, standard deviation, percentiles, of the amplitude of blade response leaving only comprehensive Monte Carlo simulations as sole option.

Given the practical significance of the problem and the associated computational effort, a large number of papers have been devoted in the last 50 years to the understanding and prediction of the effects of mistuning. Much of the early literature on this topic focused on the phenomenological aspects of blade free and forced response in mistuned disks but also on the development of predictive approaches of the statistical distribution of the response. The deterministic problem of predicting the largest amplitude of blade that can be induced by mistuning of either finite or arbitrary magnitude has also received sporadic attention. However, the rapid increase in computational capabilities in the mid 1990's shifted the focus to the successful development of reduced order modeling strategies for single stage and later on to multi stage configurations. With such methods and computational capabilities, bladed disk designs that are less sensitive to small differences in blade properties have also been actively sought, in particular by using intentional mistuning (or detuning) of the blades. A limited review of these various aspects of mistuning research is provided in [2].

1.2 BLADED DISK MODELS

To study and compare the effects of mistuning, two bladed disk models were considered.

1: Single Degree of freedom system:

The 1st model considered was the single degree of freedom (SDOF) per sector model, as shown in Figure 1, in which each sector, blade and disk, is modeled as having only 1 degree of freedom. This model is clearly an oversimplified one but it has been used in a large number of past investigations and thus is well characterized from the standpoint of mistuning. The values of the different structural properties of the blades were as follows. The stiffness of the tuned blades was selected to be k_t = 430000 *N/m*, the mass of each blade as m = 0.0114 kg, the damping ratio of the sector was chosen as 1% and the blade to blade coupling stiffness as k_C = 45430 N/m. The number of blades on the disk was taken to be N = 24.

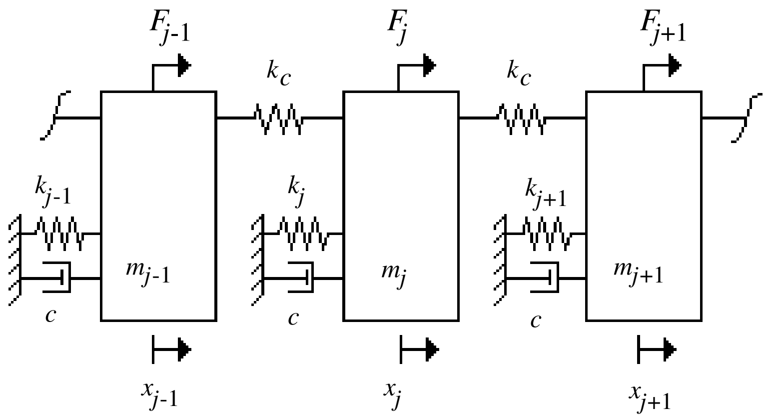

Figure 1.1.Single Degree of Freedom per Sector Bladed Disk Model.

2: Multi degree of freedom Reduced Order Model:

The 2ndmodel considered was the 12 bladed disk (referred to as blisk, a contraction of bladed-disk to highlight the single piece construction) shown in Fig. 2a for the full finite element model and in Fig. 2b for a representative sector. This system, which is a reduction to 12 blades of the disk originally modeled in [3], was analyzed both directly from the finite element model (Nastran) and using a reduced order model derived by using the University of Michigan code REDUCE v2.2 [4]. Each sector of the finite element model was constructed using 543 disk nodes and 210 blade nodes with 3 degrees of freedom each, resulting in a total of 27108 degrees of freedom for the full disk. The reduced order model was built using set of 60 disk-induced modes and 8 cantilevered blade modes for each blade, resulting in a total of 156 degrees of freedom. A damping ratio of 0.1% of critical was considered for all modes.

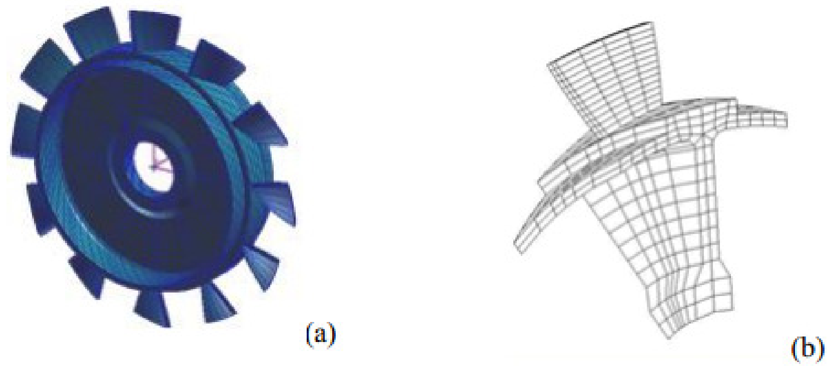

Figure 1.2. Blisk Model. (a) Full Model, (b) Single Sector Finite Element Mesh.

The natural frequencies of tuned bladed disks are usually presented in a figure, plotted vs. the number of nodal diameters to which they are associated. This plot is presented in Fig. 1.3 for the blisk of Fig. 1.2, each marker corresponding to a particular frequency. Also shown on this figure are the coupling indices [5] associated with each resonance. These indices provide a measure of the blade-disk coupling at a particular resonance. Specifically, a coupling index of zero is a blade mode in which there is no participation from the disk while a coupling index of one is indicative of a mode where the blade moves as a rigid extension of the disk, i.e. a disk dominated mode. Further discussion of the coupling index will be presented in Chapter 3. Note on Fig. 1.3 that the high coupling index modes, i.e., the disk modes, follow a rather quadratic behavior vs. number of nodal diameters while the blade dominated ones of small coupling indices are nearly constant vs. this number. When these fictitious lines intersect near an integer number of nodal diameters, a veering is obtained in which the two modes have a mix of disk and blade motions and intermediate values of the coupling index.

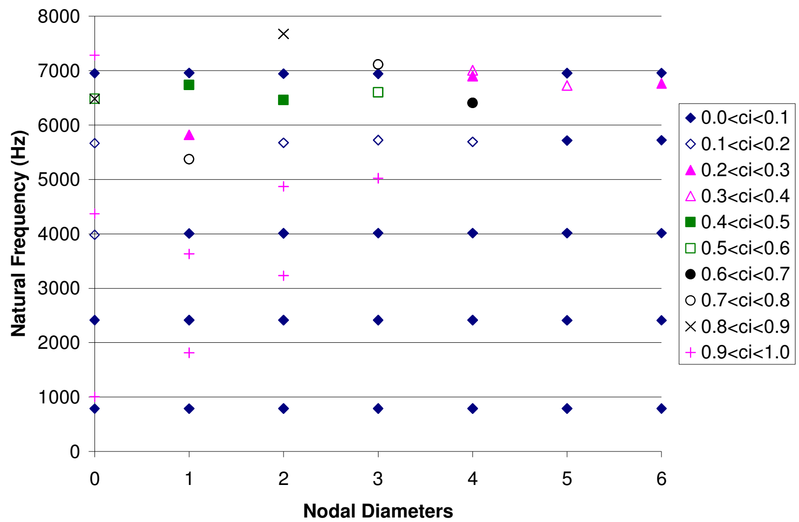

Figure 1.3.Natural Frequencies vs. Number of Nodal Diameters, Blisk Model.

A blade overall response was defined as the norm of the 8 generalized coordinates of the 8 blade modes for every blade in the reduced order model and as the norm of the 630 nodal displacements in the full finite element model.

Often defined in mistuning analyses is the amplification factor which was defined as the ratio of the maximum response of the mistuned and tuned systems taken over all the blades in the disk and over the frequency band of interest. For the blisk, this amplification factor was determined using the overall blade response.

1.3 HARMONIC MISTUNING

Harmonic mistuning refers to a particular mistuning in which the blade properties (mass, stiffness, etc.) vary harmonically around the disk, i.e., as $\beta \cos\left[2\pi s\left(j-1\right)/N\right]$

where β is the amplitude of mistuning, *i* is the blade number, *s* is the harmonic of mistuning and *N* is the number of blades. Harmonic mistuning has been considered in a very limited number of investigations, [5,6] most notably, as a simple mistuning model to derive some qualitative and quantitative information on the behavior of a bladed disk to the more characteristic random mistuning. The motivation for this form of mistuning is the parallel between the equations for a response of the mistuned bladed disk, written as a function of the angle θ, and the equations of parametrically excited vibrating systems, written as a function of time. As an example, consider the ring model of [6], see Fig. 1.4, as a simple bladed disk model. As shown in [6], its mode shapes $U(\theta)$ are solution of the equation

$$\frac{d^2U(\theta)}{d\theta^2} + [\alpha + \gamma\, k(\theta)]\, U(\theta) = 0 \tag{1.1}$$

which is identical (except for the boundary conditions vs. initial conditions) to parametrically excited systems. In these systems, the case of a harmonic variation of the parameters leading to the Mathieu equation is known to provide significant qualitative perspective on the system response.

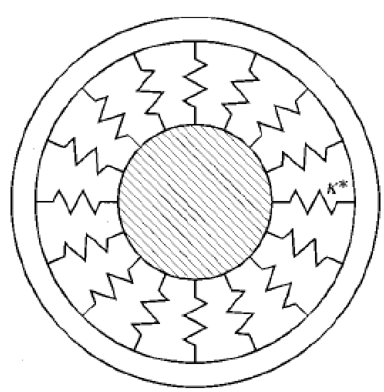

Figure 1.4. Ring Model of Bladed Disk [6].

A significant advantage of harmonic mistuning lies in that the computation of its response is expedient in comparison of the lengthy Monte Carlo simulations. A key question however is whether this response can be useful in assessing the response obtained with random mistuning. This issue received an initial assessment in [5]; some quantitative agreement was found at low mistuning levels between harmonic and random mistuning on the single degree of freedom model of Fig. 1.1 in single frequency excitation. It was shown that the most important harmonic at those low mistuning levels is $s = 2\,r$ where r is the engine order of the excitation.

The insightful work of [6] provided significant clarifications of the observations of [5] and detailed the features of the response of the ring model of Fig. 1.4. Through a first order perturbation, it was shown in [6] that:

(a) the natural frequencies of a harmonically mistuned disk are those of the tuned system except for those associated with p nodal diameters where $s = 2p$.

(b) harmonic mistuning distorts all mode shapes inducing fluctuations of them around the disk in the form of sine and cosine of $(s-p)\theta$ and $(s+p)\theta$ of magnitudes inversely proportional to $(s-2p)$ and $(s+2p)$, respectively. That is, the mode with number of nodal diameters close to $s = 2p$ are more significantly distorted than those away from this condition. This distortion implies that an rth engine order excitation will no longer excite only the $p = r$ nodal diameters modes but will excite the entire families $s - p = r$ and $s + p = r$, i.e., $p = s - r$ and $p = r - s$.

On the basis of these observations, the mechanism for increased response at low mistuning levels was related to the split of the repeated modes corresponding to $s = 2p$ as the modal force induced by modal distortion is then small. When the natural frequencies are repeated, the modes are only defined up to a linear combination (or rotation in this case) of each other and thus the response to a particular excitation can always be construed as originating from one mode with the other being appropriately rotated to induce a zero modal force. When a split of frequency occurs, the modes become locked in the structure and each one induces a peak: the one originally with large modal force being most significant. As the frequency split increased, the two modes induce more equal contributions to the response which increases as long as a single peak results. As demonstrated in [7], the largest response obtained in this manner occurs right before the peak separates into two distinct ones, see Fig. 1.5. As the split continues to increase, the peaks become more and more separated, influence each other less, and the maximum response decreases.

Thus, for small enough mistuning, the amplification results from the frequency split of the $p = r$ nodal diameters modes induced by the harmonic $s = 2\ r$ (as shown in [5]). This phenomenon is dominant until the peaks induced by these two modes separate from each other. For larger mistuning levels, other harmonics s play the dominant role, primarily those close to s = 2 r because of their increase distortion level.

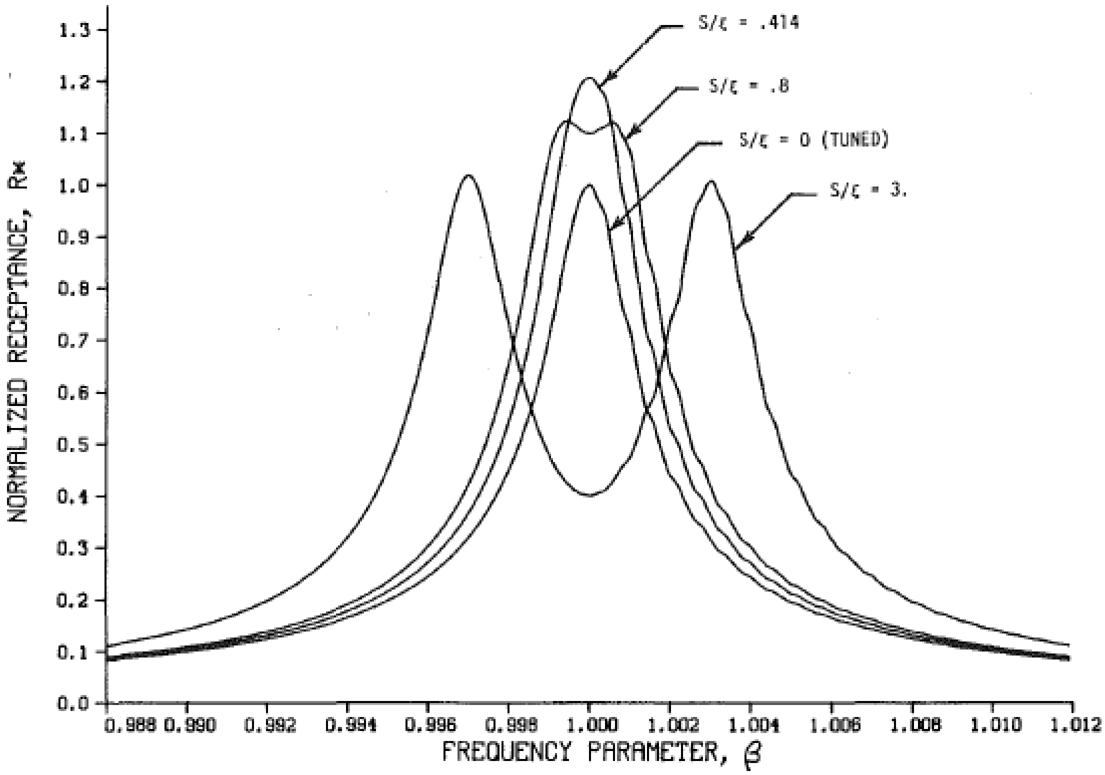

Figure 1.5. Variation of Peak Amplitude Induced by the Splitting of a Pair of Natural Frequencies [7].

1.4 YOUNG'S MODULUS AND GEOMETRIC MISTUNING

While mistuning has always been recognized as induced by blade to blade changes of material properties and/or geometry, the latter is the one which has almost consistently been considered in the past, at least until rather recently. Moreover, the material property variations that have been considered focus on Young's modulus. A practical reason for this choice is linked to the availability of data. Vibration tests of blades from which mistuning can be identified typically provide only a few frequencies, more challenging was obtaining mode shape data, and thus Young's modulus provides an easily identifiable model from experiments as it involves only a scalar parameter per blade. A similar reason is encountered in the context of modeling random mistuning, until the introduction of the nonparametric approach [8], it was challenging to develop a stochastic model of the blade properties that involves random variations of mode shapes. A turning point in the open literature has been the publication of data obtained with a Coordinates Measurement Machine (CMM) [9] which has led to the modeling of the variations in blade geometry as a sum of random amplitudes multiplied by deterministic functions consistently with a Karhunen-Loeve representation of the geometry fluctuation field [9,10,12]. Using such a model or actual blade measurements [11,13] has led to an assessment of the effects of geometry mistuning. The comparison of these effects with those resulting from a Young's modulus mistuning has surprisingly received little attention, having been addressed briefly only in [13].

CHAPTER 2

PERTURBATION

2.1 INTRODUCTION

This section discusses the possibility of applying perturbation methods to find an approximate response of mistuned bladed disks. For small enough mistuning levels, perturbation methods may be applicable to analyze the changes in frequencies, mode shapes and forced response for both the blade alone (considered cantilevered) and for the entire disk. Perturbation methods are usually less computationally demanding than their full counterparts but have a well-defined, often small, radius of convergence. Specifically, this technique is appropriate when the blade-disk coupling and damping are large enough for the radius of convergence to include the levels of mistuning of practical interest [14,16]. This method also works with smaller damping ratios but with a significant blade-disk coupling and modification of the method leading to increase in complexity. In case of weak blade-disk coupling (for e.g. in case of axial machinery for low frequency and/or large number of nodal diameter resonances) the mistuned disk response is then dominated by localization and thus an alternate perturbation approach was formulated [14,15] that assumes the blade-disk coupling to be small. Again, this method (the modified perturbation method) does provide reliable prediction of the response provided that the damping and the mistuning are large enough.

Focusing on appropriately small levels of mistuning, the present chapter reviews and assesses the applications of perturbation methods to first order techniques to the determination of the natural frequencies, mode shapes, and response of blades alone and entire disks. In the former case, the natural frequencies are assumed to be all well separated while in the latter the pair of tuned natural frequencies focused on is considered well separated of all others.

2.2 SINGLE MODE PERTURBATION

Denote by K and M the stiffness and mass matrices of the original system, a blade here, and the corresponding mistuned system matrices by $\hat{K}$ and $\hat{M}$. It is desired to determine the resulting change in the response of the system to a force $\underline{F} = \underline{F}e^{i\omega t}$ when it is assumed to have small classical damping.

Assuming that a single mode is dominant, the response of the perturbed system is approximately given by

$$\underline{\hat{X}} = \hat{q}\underline{\hat{\psi}} \tag{2.1}$$

Here, $\hat{q}$ is the modal (generalized) coordinate, $\underline{\hat{\psi}}$ is the mode shape of the mode at resonance and $\hat{X}$ is the amplitude of response. The mode shape of the perturbed satisfies the eigen-vector equation

$$\hat{K}\underline{\hat{\psi}} = \hat{\lambda}\hat{M}\underline{\hat{\psi}} \tag{2.2}$$

with the normalization $\underline{\hat{\psi}}^T \hat{M}\underline{\hat{\psi}} = 1$. Setting up the perturbation problem, the matrices are first separated into tuned and mistuned components as follows

$$\hat{K} = K + \Delta K \tag{2.3}$$

$$\hat{M} = M + \Delta M \tag{2.4}$$

$$\underline{\hat{\psi}} = \underline{\psi} + \Delta\underline{\psi} \tag{2.5}$$

$$\hat{\lambda} = \lambda + \Delta\lambda \tag{2.6}$$

Introducing Eqs. (2.3) - (2.6) in Eq. (2.2) and retaining only the 1st order terms yields

$$\hat{K}\underline{\hat{\psi}} = K\underline{\psi} + \Delta K\underline{\psi} + K\Delta\underline{\psi} \tag{2.7}$$

$$\hat{\lambda}\hat{M}\underline{\hat{\psi}} = \lambda M\underline{\psi} + \Delta\lambda M\underline{\psi} + \lambda\Delta M\underline{\psi} + \lambda M\Delta\underline{\psi} \tag{2.8}$$

Since, $K\underline{\psi} = \lambda M\underline{\psi}$ and $\hat{K}\underline{\hat{\psi}} = \hat{\lambda}\hat{M}\underline{\hat{\psi}}$, the above equations can be written as

$$\Delta K\underline{\psi} + K\Delta\underline{\psi} = \Delta\lambda M\underline{\psi} + \lambda\Delta M\underline{\psi} + \lambda M\Delta\underline{\psi}$$

or

$$(K - \lambda M)\Delta\underline{\psi} = \Delta\lambda M\underline{\psi} + (\lambda\Delta M - \Delta K)\underline{\psi} \tag{2.9}$$

Turning next to the normalization condition, it is found that

$$\underline{\hat{\psi}}^T\hat{M}\underline{\hat{\psi}} = \underline{\psi}^T M\underline{\psi} + \Delta\underline{\psi}^T M\underline{\psi} + \underline{\psi}^T\Delta M\underline{\psi} + \underline{\psi}^T M\Delta\underline{\psi} = 1 \tag{2.10}$$

Since $\underline{\hat{\psi}}^T\hat{M}\underline{\hat{\psi}} = 1$, $\underline{\psi}^T M\underline{\psi} = 1$ and $\underline{\psi}^T M\,\Delta\underline{\psi} = \Delta\underline{\psi}^T M\underline{\psi}$, Eq. (2.10) reduces to

$$2\Delta\underline{\psi}^T M\underline{\psi} + \underline{\psi}^T\Delta M\underline{\psi} = 0 \text{ or } \Delta\underline{\psi}^T M\underline{\psi} = -\frac{1}{2}(\underline{\psi}^T\Delta M\underline{\psi}) \tag{2.11}$$

Now, left multiplying Eq. (2.9) by $\underline{\psi}^T$, it is found that

$$\Delta\lambda = (\underline{\psi}^T\Delta K\underline{\psi}) - \lambda(\underline{\psi}^T\Delta M\underline{\psi}) \tag{2.12}$$

The change in eigen-value $\Delta\lambda$ can be determined from the above equation since all the other variables are known. Plugging then the calculated $\Delta\lambda$ from equation (2.12) into equation (2.9), leads to the estimation $\Delta\underline{\psi}$. In this regard, note that the matrix $K - \lambda M$ is singular and thus $\Delta\underline{\psi}$ can only be determined to within a multiple of the null space of $K - \lambda M$, i.e. $\underline{\psi}$. The solution procedure followed here was to eliminate the row and columns of $K - \lambda M$ corresponding to the largest component of $\underline{\psi}$, solve for the corresponding reduced size vector $\Delta\underline{\psi}$, then determine the missing component to satisfy the normalization condition of Eq. (2.11)

The response of the system is given by Eq. (1) where the generalized coordinate $\hat{q}$ is given by:

$$\hat{q} = \frac{(\underline{\psi} + \Delta\underline{\psi})^T \hat{F}}{2\zeta[\lambda + \Delta\lambda + \lambda(\underline{\psi}^T \Delta M\, \underline{\psi})]} \tag{2.14}$$

or

$$\hat{q} = q + \frac{\Delta\underline{\psi}^T \underline{F}}{2\zeta\lambda} + \frac{\underline{\psi}^T \underline{F}}{2\zeta\lambda}[-\frac{\Delta\lambda}{\lambda} - \underline{\psi}^T \Delta M\, \underline{\psi}] \tag{2.15}$$

The system chosen for validation, was a cantilevered blade alone model corresponding to the blades of the blisk of Fig. 1.2. The finite element model has 210 nodes each with 3 degrees of freedom. The perturbation of mass and stiffness was induced by perturbing the geometry of the blade at a single node. The following figures represent the comparison of the perturbation solution for differences in frequency, mode shape and response of the unperturbed vs. perturbed system as compared to the full eigen-value analysis. The red dots represent the actual eigen-value analysis and the black lines are the perturbation solutions. All figures are plotted with respect to the degrees of freedom of the blade. A very good match is obtained when considering eigen-value, eigen-vector, and response changes.

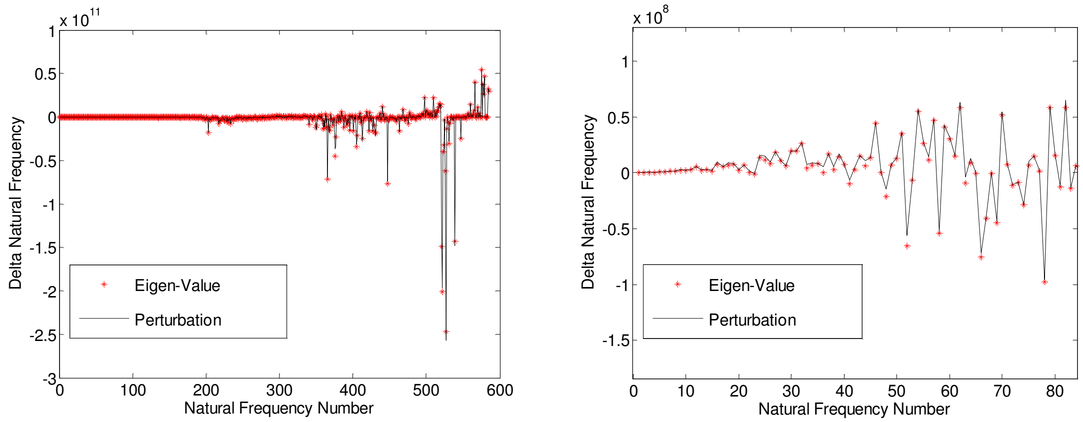

(a) (b)

Figure 2.1. (a) Comparison of Eigen-Value Changes $\Delta\lambda$ between Perturbation Solution and Full Eigen-Value Analysis for the Ensemble of Modes. (b) Same as (a), Zoomed.

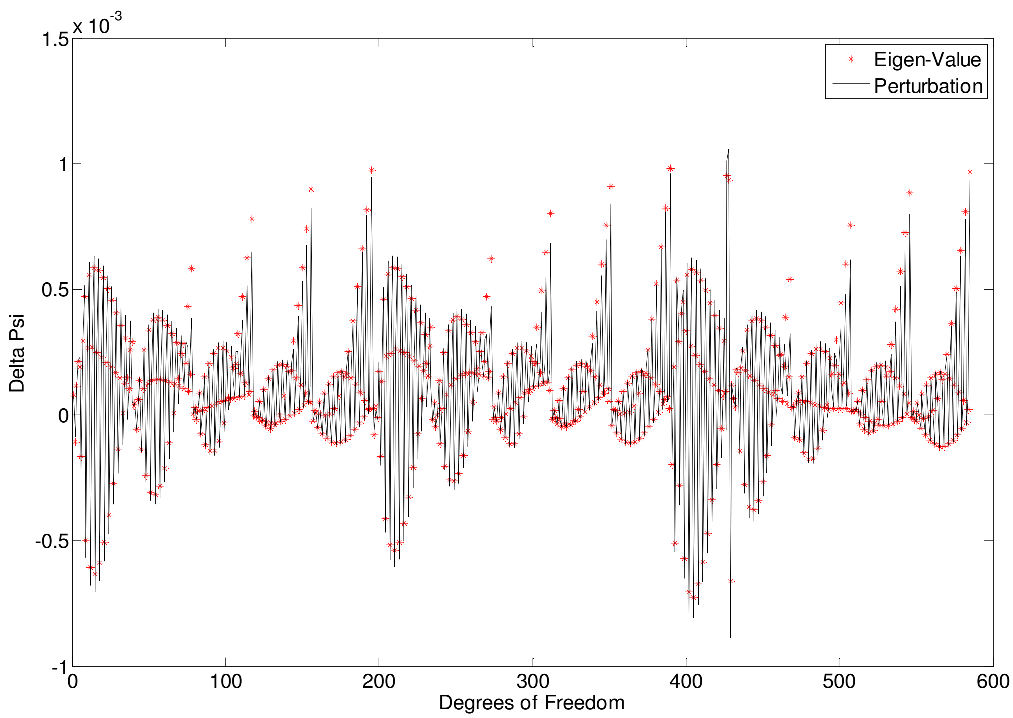

Figure 2.2. Comparison of Eigen-Vector Change $\Delta\underline{\psi}$ between Perturbation Solution and Full Eigen-Value Analysis for a Particular Mode.

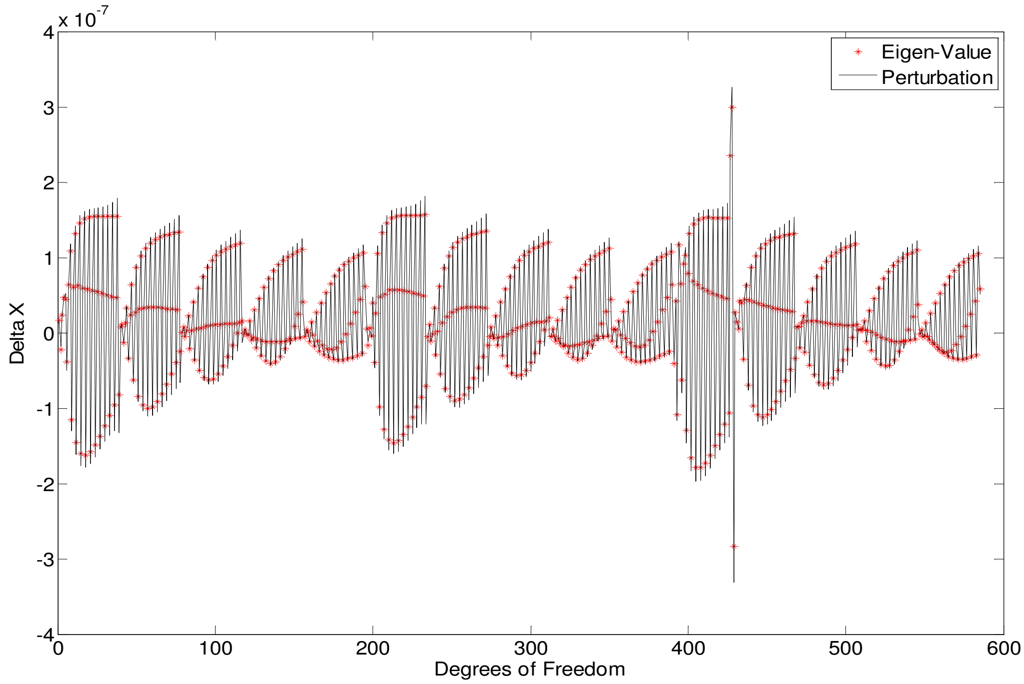

Figure 2.3. Comparison of Forced Response Change $\Delta \underline{X}$ between Perturbation Solution and Full Eigen-Value Analysis.

2.3 REPEATED MODE PERTURBATION

In cyclosymmetric systems, such as bladed disks, there are repeated natural frequencies and thus the perturbation analysis of the previous section must be modified. Denote by K_0 and M_0 are the stiffness and mass matrices of the tuned system. It has 2 modes $\underline{\psi}_1$ and $\underline{\psi}_2$ associated with the frequencies $\lambda_i = \lambda_0$. The unperturbed eigen-value problems is

$$K_0 \underline{\psi}_i = \lambda_i M_0 \underline{\psi}_i \tag{2.16}$$

Consider next the perturbed system:

$$(K_0 + \Delta K)\underline{\phi} = (\lambda_0 + \Delta\lambda)(M_0 + \Delta M)\underline{\phi} \tag{2.17}$$

At the contrary of the single mode perturbation, one cannot simply assume that the modes $\underline{\phi}$ are small perturbations of the modes $\underline{\psi}_i$ because these modes are not uniquely defined; any linear combination of $\underline{\psi}_1$ and $\underline{\psi}_2$ is also a bona fide solution of Eq. (2.16). It can however be assumed that $\underline{\phi}$ are small perturbations of an appropriate linear combinations of $\underline{\psi}_1$ and $\underline{\psi}_2$. That is, the 2 perturbed mode shapes are expressed as

$$\underline{\phi}_1 = \underline{\tilde{\psi}}_1 + \Delta\underline{\psi}_1 \tag{2.18}$$

$$\underline{\phi}_2 = \underline{\tilde{\psi}}_2 + \Delta\underline{\psi}_2 \tag{2.19}$$

where:

$$\underline{\tilde{\psi}}_1 = a_{11}\underline{\psi}_1 + a_{12}\underline{\psi}_2 \tag{2.20}$$

$$\underline{\tilde{\psi}}_2 = a_{21}\underline{\psi}_1 + a_{22}\underline{\psi}_2 \tag{2.21}$$

Proceeding as in the previous section, introduce the perturbation in stiffness and mass matrices and their corresponding perturbation in eigen-value and eigen-vector. Then,

$$(K_0 + \Delta K)\underline{\phi}_i = (\lambda_0 + \Delta\lambda)(M_0 + \Delta M)\underline{\phi}_i \tag{2.22}$$

Neglecting 1st order terms and expanding leads to

$$K_0\Delta\underline{\psi}_i + \Delta K\underline{\tilde{\psi}}_i = \Delta\lambda_0 M_0\underline{\tilde{\psi}}_i + \lambda_0\Delta M\underline{\tilde{\psi}}_i + \lambda_0 M_0\Delta\underline{\psi}_i \tag{2.23}$$

Rearranging terms, it is found that

$$(K_0 - \lambda_0 M_0)\Delta\underline{\psi}_i = \Delta\lambda_i M_0\underline{\tilde{\psi}}_i + \lambda_0\Delta M\underline{\tilde{\psi}}_i - \Delta K_0\underline{\tilde{\psi}}_i \tag{2.24}$$

Pre-multiplying by $\underline{\tilde{\psi}}_i^T$ as in the previous section yields

$$\underline{\tilde{\psi}}_i^T(K_0 - \lambda_0 M_0)\Delta\underline{\psi}_i = \Delta\lambda_i\underline{\tilde{\psi}}_i^T M_0\underline{\tilde{\psi}}_i + \lambda_0\underline{\tilde{\psi}}_i^T\Delta M\underline{\tilde{\psi}}_i - \underline{\tilde{\psi}}_i^T\Delta K_0\underline{\tilde{\psi}}_i \tag{2.25}$$

Since, $(K_0 - \lambda_0 M_0) = 0$ and $\underline{\tilde{\psi}}_i^T M_0\underline{\tilde{\psi}}_i = 1$ assuming mass normalized eigen-vectors, one obtains

$$\Delta\lambda i = \underline{\tilde{\psi}}_i{}^T (\Delta K - \lambda_0 \Delta M)\underline{\tilde{\psi}}_i \tag{2.26}$$

The change in eigen-value $\Delta\lambda_i$ can be solved from Eq. (2.26).Reintroducing this result in Eq. (2.24) provides a means to solve for $\Delta\underline{\psi}_i$. However, $K_0 - \lambda_0 M_0$ has two zero eigen-values corresponding to eigen-vectors $\underline{\tilde{\psi}}_1$ and $\underline{\tilde{\psi}}_2$. To avoid an unbounded solution, it is necessary that the right-hand-side of Eq. (2.24) be orthogonal to $\Delta\underline{\tilde{\psi}}_1$ and $\Delta\underline{\tilde{\psi}}_2$. Since

$$\underline{\tilde{\psi}}_1{}^T (K_0 - \lambda_0 M_0) = \underline{\tilde{\psi}}_2{}^T (K_0 - \lambda_0 M_0) = 0 \tag{2.27}$$

it is necessary to have

$$\underline{\tilde{\psi}}_j{}^T (\Delta\lambda_i M_0 \underline{\tilde{\psi}}_i + \lambda_0 \Delta M \underline{\tilde{\psi}}_i - \Delta K \underline{\tilde{\psi}}_i) = 0 \tag{2.28}$$

for *i*, *j* = 1,2. For *i* = *j*, this condition reduces to Eq. (2.26). However, for *j* = 2 and *i* =1, it is required that

$$\underline{\tilde{\psi}}_2{}^T (\Delta\lambda_1 M_0 \underline{\tilde{\psi}}_1 + \lambda_0 \Delta M \underline{\tilde{\psi}}_1 - \Delta K \underline{\tilde{\psi}}_1) = 0$$

or

$$\Delta\lambda_1 \underline{\tilde{\psi}}_2^T M_0 \underline{\tilde{\psi}}_1 + \underline{\tilde{\psi}}_2{}^T (\lambda_0 \Delta M - \Delta K)\underline{\tilde{\psi}}_1 = 0$$

Since $\underline{\tilde{\psi}}_2{}^T M_0 \underline{\tilde{\psi}}_1 = 0$ by orthogonality of the eigen-vectors, the above relation holds if the coefficients $a_{11}, a_{12}, a_{21}, a_{22}$ are such that:

$$\underline{\tilde{\psi}}_2{}^T (\Delta K - \lambda_0 \Delta M)\underline{\tilde{\psi}}_1 = 0 \tag{2.29}$$

To maintain the normalization and orthogonality of the modes $\underline{\tilde{\psi}}_1$ and $\underline{\tilde{\psi}}_2$, it is required that

$$\underline{\tilde{\psi}}_1{}^T M_0 \underline{\tilde{\psi}}_1 = 1 \tag{2.30}$$

$$(a_{11}\underline{\psi}_1+a_{12}\underline{\psi}_2)M_0(a_{11}\underline{\psi}_1+a_{12}\underline{\psi}_2)=1 \quad (2.31)$$

Therefore,

$$a_{11}^2+a_{12}^2=1 \text{ and similarly } a_{21}^2+a_{22}^2=1 \quad (2.32)$$

Since $\underline{\tilde{\psi}}_2^T M_0 \underline{\tilde{\psi}}_1=0$, $(a_{11}\underline{\psi}_1+a_{12}\underline{\psi}_2)M_0(a_{21}\underline{\psi}_1+a_{22}\underline{\psi}_2)=0$. Hence,

$$a_{11}a_{12}+a_{21}a_{22}=0 \quad (2.33)$$

These relations admit the solution:

$$a_{11}=a_{12}=\cos\varphi \text{ and } a_{21}=a_{22}=\sin\varphi \quad (2.34)$$

The angle φ is determined as follows. Let

$$h_{ij}=\underline{\psi}_i^T(\Delta K-\lambda_0\Delta M)\underline{\psi}_j \quad (2.35)$$

then

$$a_{21}a_{11}h_{11}+a_{21}a_{12}h_{12}+a_{22}a_{11}h_{21}+a_{22}a_{12}h_{22}=0 \quad (2.36)$$

Using Eq. (2.34) and solving yields

$$\tan\varphi=\frac{2h_{21}}{h_{11}-h_{22}} \quad (2.37)$$

The angle φ can be determined from the above equation with coefficients h_{ij} calculated from Eq. (2.35). The difference of eigen-value $\Delta\lambda$ is then from Eq. (2.26) and the difference of modes from Eq. (2.23) using first an elimination of two rows and columns, as described in the previous section.

Since, there are repeated modes, the response in the perturbed case is given by

$$\underline{\hat{X}}=\frac{\underline{\phi}_1^T\underline{F}e^{i\omega t}}{\hat{\omega}_1^2-\omega^2+i2\zeta\hat{\omega}_1\omega}\underline{\phi}_1+\frac{\underline{\phi}_2^T\underline{F}e^{i\omega t}}{\hat{\omega}_2^2-\omega^2+i2\zeta\hat{\omega}_2\omega}\underline{\phi}_2 \quad (2.38)$$

while it was for the unperturbed system

$$\underline{X} = \frac{\underline{\psi_1}^T \underline{F} e^{i\omega t}}{\omega_1{}^2 - \omega^2 + i2\zeta\omega_1\,\omega}\underline{\psi_1} + \frac{\underline{\psi_2}^T \underline{F} e^{i\omega t}}{\omega_2{}^2 - \omega^2 + i2\zeta\omega_2\,\omega}\underline{\psi_2} \tag{2.39}$$

The validation of this perturbation solution was carried out on the reduced order model of the blisk of Fig. 1.2. The perturbation used was Young's mistuning which results in the splitting of the natural frequencies from the repeated pair of the tuned case. It was then convenient for validation to focus on the split between the two frequencies shown in Fig. 2.4 vs. mistuning level. Clearly, the perturbation provides the correct solution for small enough mistuning levels. Comparisons of the changes in mode shape and response in such conditions are excellent, see Figs 2.5 and 2.6, demonstrating the applicability of the perturbation method.

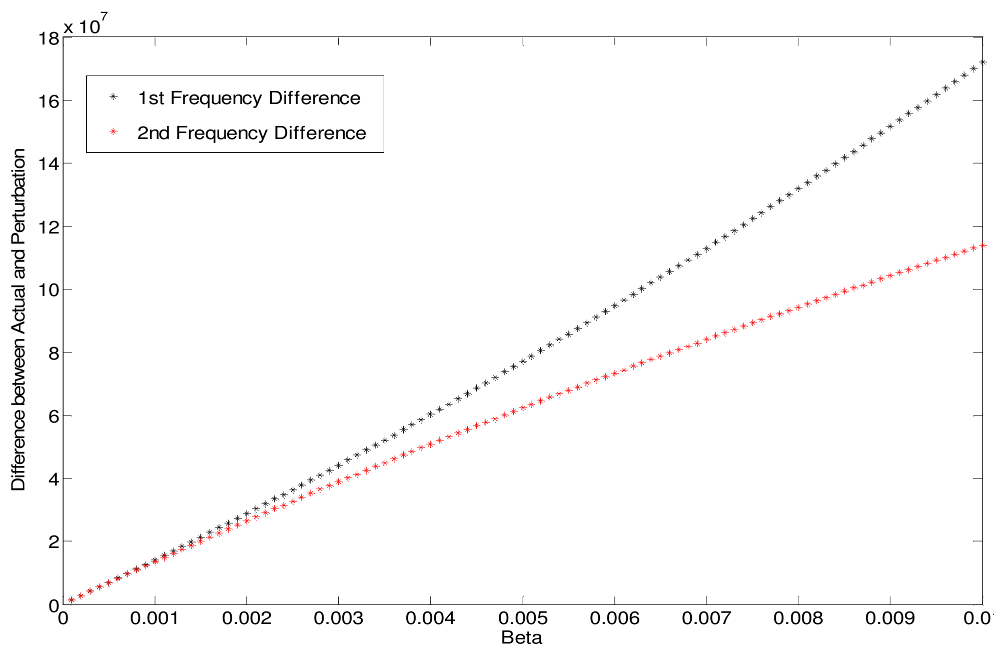

Figure 2.4.Comparisonof the Eigen-Value Change $\Delta\lambda$ between Perturbation Solution and Full Eigen-Value Analysis as a Function of the Mistuning Level.

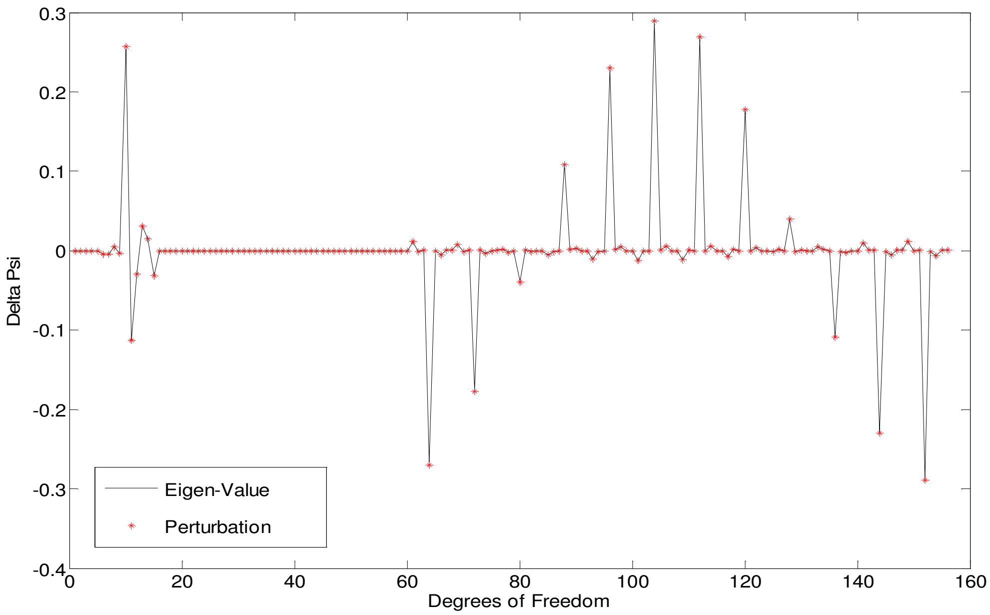

Figure 2.5. Comparison of the Mode Shape Change $\Delta\underline{\psi}$ between Perturbation Solution and Full Eigen-Value Analysis.

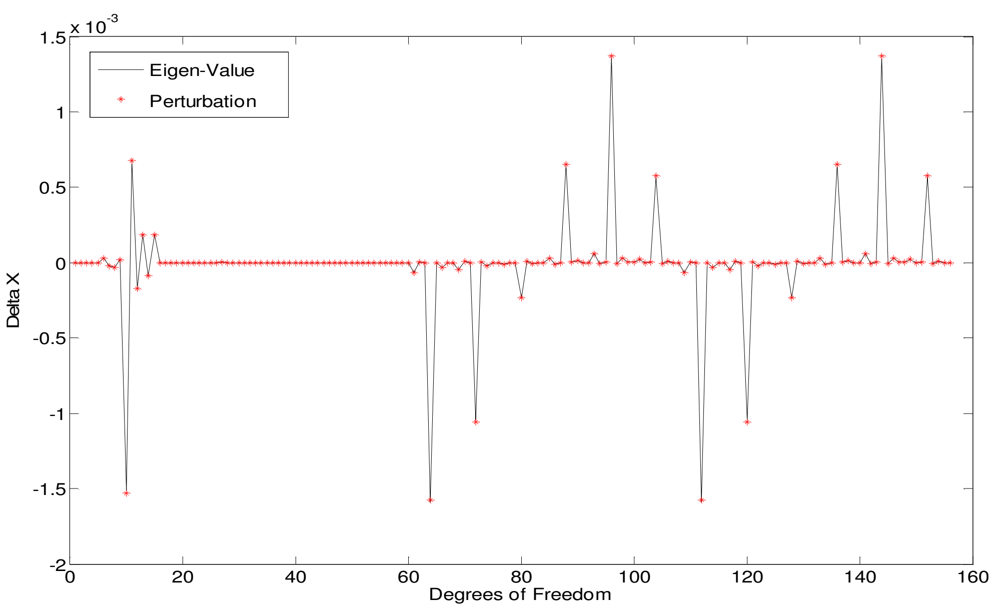

Figure 2.6. Comparison of the Change in Response $\Delta\underline{X}$ between Perturbation Solution and Full Eigen-Value Analysis.

CHAPTER 3

HARMONIC MISTUNING

3.1 INTRODUCTION AND PLAN

The investigations on the effects of harmonic mistuning reported in Chapter 1, i.e., [5,6], were carried out at a transition time. Before then, the mistuning analyses were typically carried out on small bladed disk models and were focused on both qualitative understanding and quantitative predictions while after that transition, they were rather solely aimed at the latter. This poor timing is one reason for the lack of impact of these publications on the current mistuning research. Another likely reason is that they both focused only on single degree of freedom per sector model and thus left unanswered questions on their applicability to more complex bladed disk models. This lack of results represented a key motivation for the present investigation.

The following sections will focus first on a revisit of the single degree of freedom model which will bring some new observations, then on an assessment of a modified model which includes decaying exponential and harmonic mistuning. Next, complex bladed disk models will be considered both in isolated resonance and tight veering conditions.

3.2REVISIT OF THE SINGLE DEGREE OF FREEDOM PER BLADE MODEL

The analyses of [5,6] provided good support for the consideration of harmonic mistuning as first estimator of its effects but both had weaknesses. The analysis of [5] focused solely on the forced response problem and moreover at the single frequency corresponding to a tuned system natural frequency. The analysis of [6] was more complete but was carried out on a continuous structure and thus did not include any potential effects induced by the periodicity of the number of blades. Clearly, one such effect is that the optimum harmonic $s = 2\ r$ should be understood modulo the number of blades, i.e., $s = N - 2\ r$, if $r > N/4$.

Focusing next on other modes $j \neq s\ /\ 2$, it was restated in Chapter 1 that the distortion of its mode shapes involves, to first order in the mistuning, harmonic terms of $j - s$ and $j + s$. These term will give rise to nonzero modal force, and thus to the appearance of the corresponding resonance in the response vs. frequency plot, when $j - s = r$ or $j - s = N - r$ and similarly when $j + s = r$ or $j + s = N - r$. Solving these equalities under the condition $s = 2\ r$ gives, in addition to the obvious solution $j = r$, a resonance condition $j = 3\ r$ or$j = N - 3\ r$. This discussion suggests that the presence of a resonance of the mode with that many nodal diameters in the close neighborhood of the one with r nodal diameters would result in an interaction between the two modes. The cases $r = N/3$ and $r = N/4$ are peculiar in this analysis as the first one yields $3\ r = N$ or 0 given the periodicity of the bladed disk while the second leads to $3\ r = 3\ N/4 = N/4 = r$ again with the periodicity. In the former case, the mode that could be excited is the 0 nodal diameter one which leads to uniform increases or decreases or response which are seldom large. In the latter case, the mode that could be excited is already the one excited and no new physics would be observed.

When the mistuning becomes large enough, the linearized analyses of [5,6] no longer apply and one must resort to full computations to determine the amplification of amplitude induced by a particular harmonic of mistuning (s) at a particular level (β). Such data can conveniently be presented on 3D plots such as shown in Fig. 3.1-3.5

obtained for the model of Fig. 1.1. Note in these figures that the behavior is indeed fully consistent with the analyses of [5,6], i.e., at small mistuning levels, the only significant harmonic is the $s = 2r$ one which peaks rapidly and decreases (see [6] for discussion based on the work of [7]). Following closely below the $s = 2r$ curve are those of the neighboring values of s. At higher level however, these curves are themselves replaced as largest across the set of harmonics by others: $s = 6$, for $r = 2$ (Fig. 3.1), $s = 9$, for $r = 3$ (Fig. 3.2), $s = 11$, for $r = 4$ (Fig. 3.3), and$s = 11$, for $r = 8$ (Fig. 3.5). Note that the plots for $r = 4$ and $r = 8$ are quite similar, most likely owing to the fact that $s = 8$ in both cases given periodicity. These sets of harmonics are strongly correlated to $s = 3r$.

Note finally that the case $r = 6$ of Fig. 3.4 gives rise to much smaller increases in amplitude of blade response as compared to those seen in other figures. This result is consistent with generally accepted, yet not fully understood, finding that resonance of $N/4$ nodal diameters are less sensitive to mistuning than other.

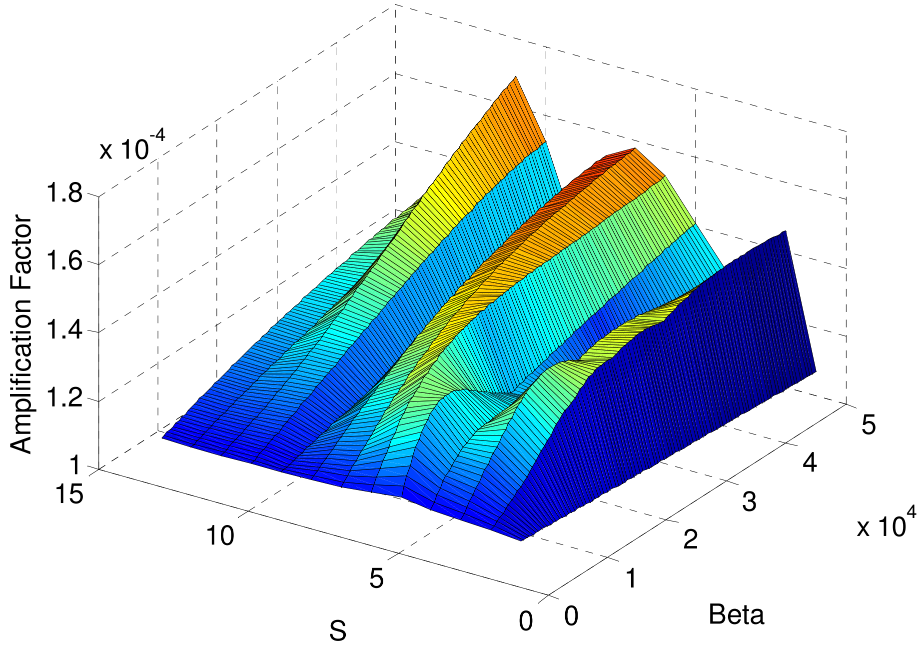

Figure 3.1. Maximum Amplitude of Blade Response in Sweep, Single Degree of Freedom per Sector Model, *r* =2.

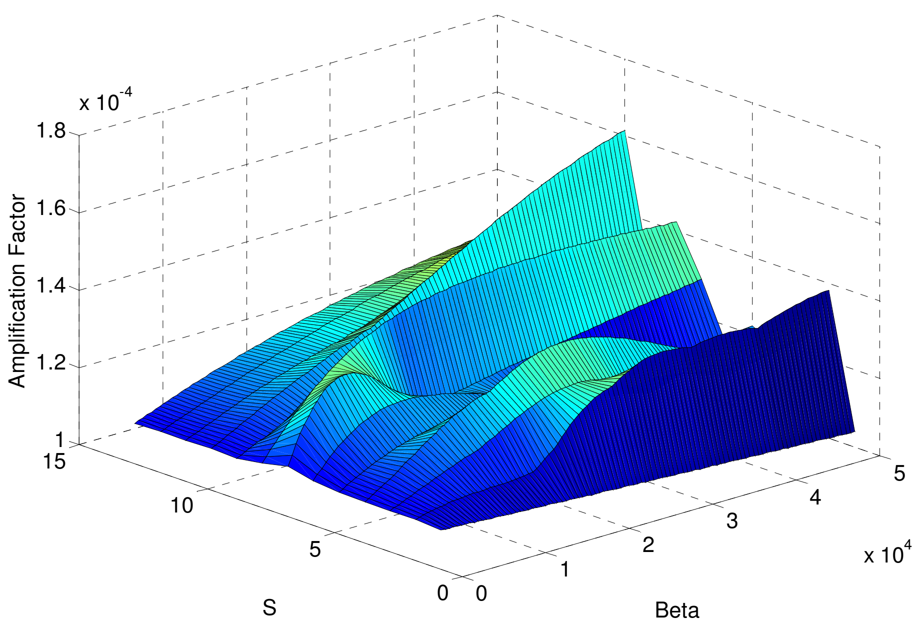

Figure 3.2. Maximum Amplitude of Blade Response in Sweep, Single Degree of Freedom per Sector Model, *r* =3.

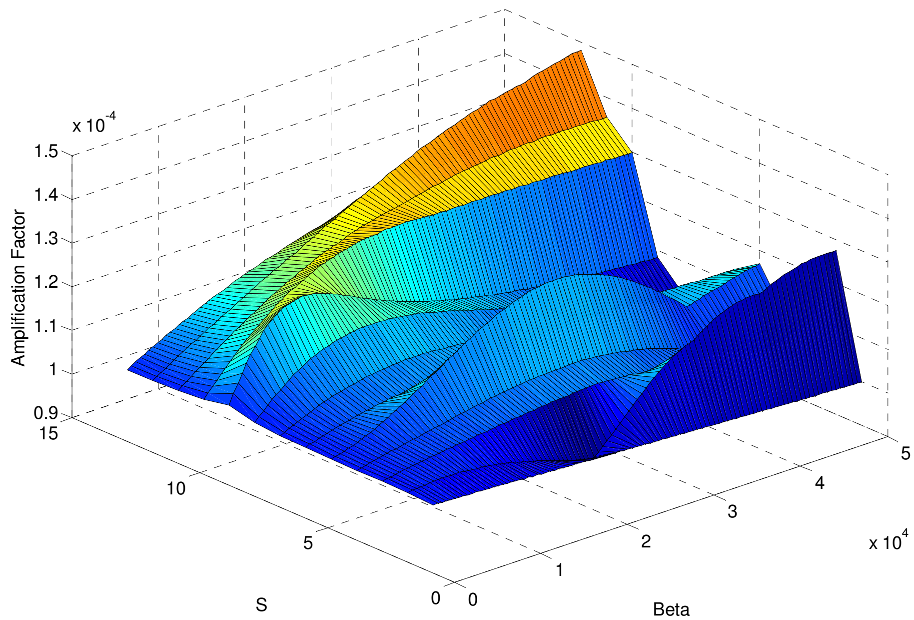

Figure 3.3. Maximum Amplitude of Blade Response in Sweep, Single Degree of Freedom per Sector Model, r =4.

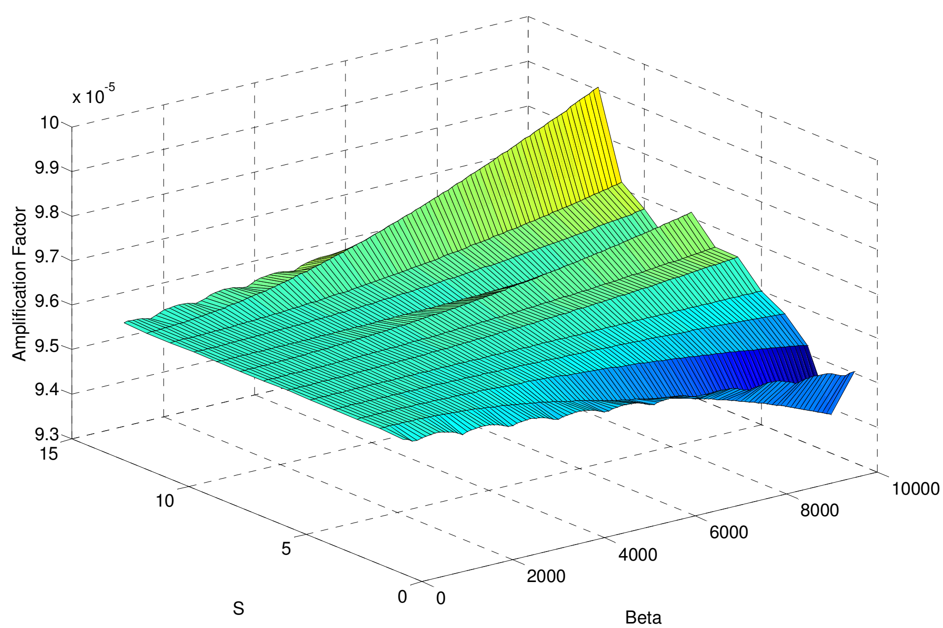

Figure 3.4. Maximum Amplitude of Blade Response in Sweep, Single Degree of Freedom per Sector Model, r =6.

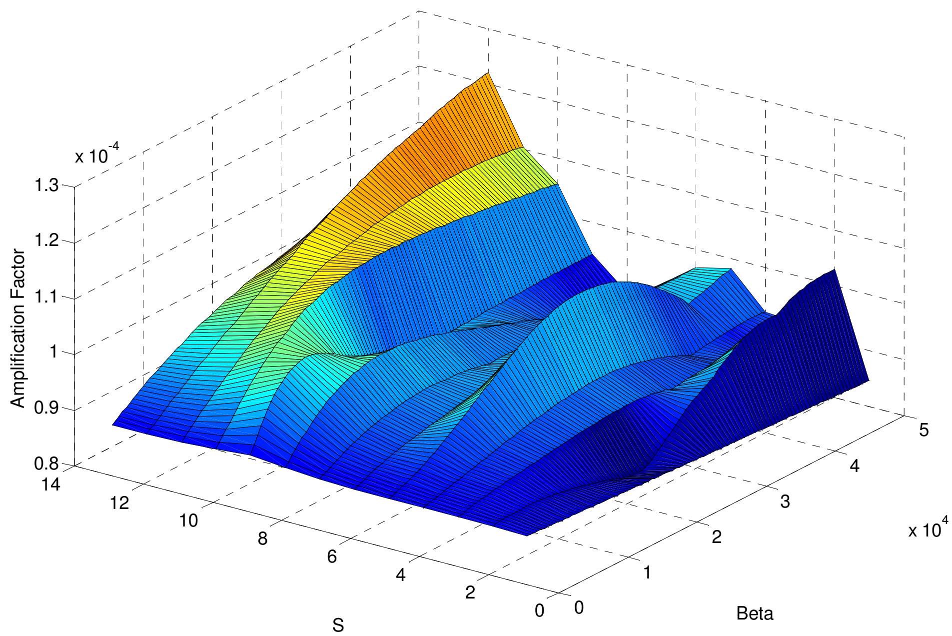

Figure 3.5. Maximum Amplitude of Blade Response in Sweep, Single Degree of Freedom per Sector Model, $r = 8$.

The frequency split of the natural frequencies corresponding to a particular number of nodal diameters p under the harmonic mistuning with $s = 2p$ is different for different values of p, depending on the coupling that exists between blade and disk. Indeed, modes in which the blades do not exhibit significant deformations, i.e., the disk modes discussed in Chapter 1, should not be affected by the change in properties and thus their natural frequencies should not split or very little. On the opposite, blade modes should have a split in their frequencies that matches the changes in the blade alone properties. These observations suggest that one could define a measure of blade-disk coupling as

$$hci = 1 - \left[\frac{\omega_p^+ - \omega_p^-}{\omega_p^0} \right] / \left[\frac{\omega_b^+ - \omega_b^-}{\omega_b^0} \right] \tag{3.1}$$

where ω_p^+ and ω_p^- are the two, high and low, natural frequencies of the *p* nodal diameter modes with harmonic mistuning $s = 2p$, ω_p^0 is the corresponding tuned frequency, and ω_b^+, ω_b^-, and ω_b^0 are their counterparts for the blade alone. The hci value, referred to here as *harmonic coupling index*, equals 0 for pure blade modes and 1 for pure disk modes.

The above definition of the harmonic coupling index is very similar to the one of the coupling index [2,19]

$$ci = 1 - \frac{\omega_p(1+\delta E) - \omega_p(1)}{\left(\sqrt{1+\delta E} - 1\right)\omega_p(1)} \tag{3.2}$$

where $\omega_p(1)$ and $\omega_p(1+\delta E)$ denote the *p* nodal diameter natural frequencies of the tuned bladed disks with blade Young's modulus equal, respectively, to its design value and to this value multiplied by the factor $1+\delta E$. Note that the increment of Young's modulus affects only the blades, not the disk.

Clearly, the ci and hci are very similar in intent but also in construction. Indeed, the coupling index corresponds to a uniform change in the blade properties which is identical to a harmonic mistuning with $s = 0$. So, the key difference between hci and ci is the harmonic of mistuning under which they are computed. Note however that the hci is a measure of coupling *pertinent to a mistuned model* while the ci is based on tuned analyses.

A comparison of hci and ci values obtained for the single degree of freedom per sector model is shown in Fig. 3.6. For this particular bladed disk model, it is seen that the hci and ci are equal (the value for *N*/4 nodal diameters is ignored because of its specificity described above). A full clarification of this property and an assessment of the hci in more complex situations will be necessary in a future research.

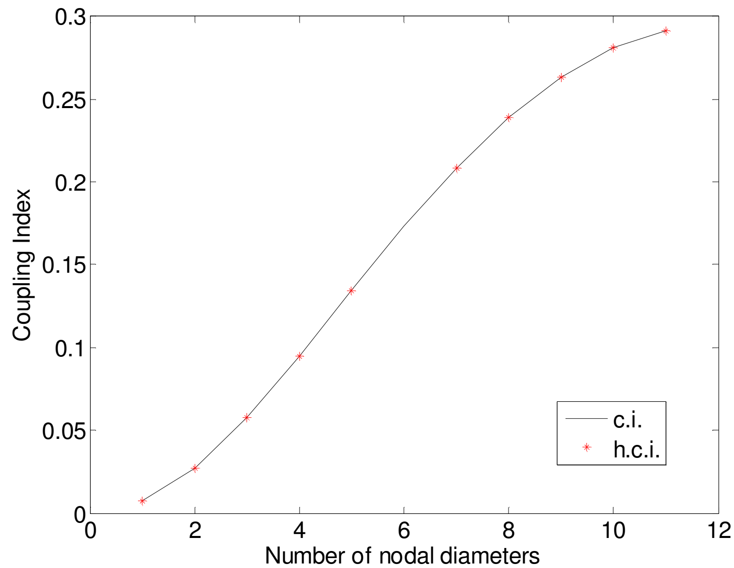

Figure 3.6. Harmonic Coupling Index (hci) and Coupling Index (ci) Values for the Single Degree of Freedom per Sector Model Vs. Number of Nodal Diameters.

While harmonic mistuning has been discussed in the context of intentional mistuning [17,18], the focus of the present effort is on unintentional mistuning which is most traditionally modeled with randomly, not harmonically, varying properties. Accordingly, it was questioned how well the maximum amplification maximized over all *s* values would compare with predictions from random mistuning. This issue is addressed in Fig. 3.6 where the red circles are the maximum amplification obtained from the harmonic mistuning analyses while the solid lines correspond to the 95th percentile of Monte Carlo analyses predicted by either sweep analysis or computations at the natural frequencies of the mistuned system. Again, for small values of the mistuning level, the harmonic mistuning provides a close quantitative estimate of the effects of random mistuning. At higher levels, the matching becomes qualitative only.

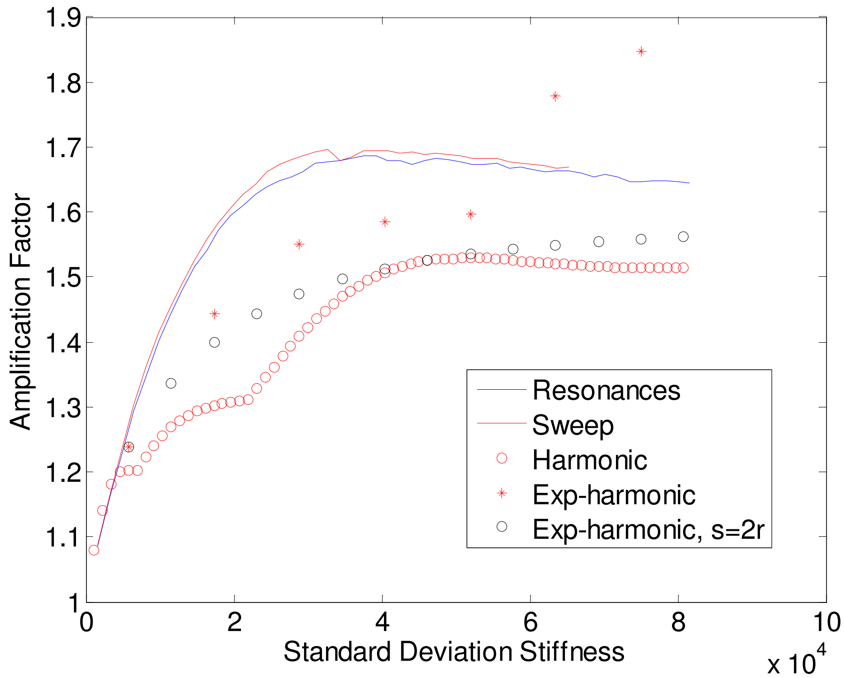

Figure 3.7. Maximum amplification of blade response for harmonic and exponential-harmonic mistuning. Single degree of freedom per sector model, $r = 3$.

As the mistuning level increases, localization increases and the blades become less and less affected by the mistuning occurring on "far away" blades. Thus, the mistuning pattern that should affect most the response of a particular blade, say blade 1, is one in which the mistuning is largest near that blade and smallest away from it to permit the propagation of the energy toward blade 1, even from far away blades. This discussion suggests considering instead the exponential-harmonic mistuning defined as (for blade 1)

$$k_j = k_t + \beta \exp[-\alpha(j-1)]\cos[2\pi s(j-1)/N]. \quad (3.3)$$

Note that this equation is valid only till the blade $j = N/2$, symmetry of the mistuning pattern is enforced for the other half of the disk. The response in sweep of the single degree of freedom system to the mistuning of Eq. (3.3) was determined for a broad range of values of the "decay" parameter α, the magnitude β, and all values of the harmonic s. Then, the maximum of these values over α and s were obtained and are plotted as the red stars in Fig. 3.7. Note that these values provide a much better fit of the quantitative behavior of the random mistuning predictions at small mistuning level and of the qualitative behavior of this curve at higher levels. Also shown on this curve is the exponential-harmonic curve corresponding to $s = 2r$ (black stars) which does quite well while needing a smaller computational effort.

Note that similar comparisons were also obtained with lower values of k_C and/or lower values of the damping (down to 0.1%) of the single degree of freedom system of Fig. 1.1 suggesting that the above results are typical.

3.3 ISOLATED RESONANCE OF THE BLISK FINITE ELEMENT MODEL

When considering a more complex bladed disk model, such as the one of the blisk of Fig. 1.2, different resonances conditions can be encountered which should be studied separately. The first case corresponds to isolated resonances of the tuned model, i.e., for the particular engine order excitation, there is only one pair of modes (one mode for $r = 0$ or $r = N/2$ for N even) excited in the frequency band of interest. The second possibility is to have two pairs of modes closely spaced; it can originate from either a veering of a disk mode with a family of blade modes or from two blade modes close to each other. This second possibility will be discussed in the ensuing section in the case of a veering.

To assess the role/influence of harmonic mistuning, Young's modulus mistuning was considered here to remove the potential effects induced by changes in blade alone mode shapes. The blisk model of Fig. 1.2 was selected for this analysis with an 1st engine order excitation (r = 1) in the range of 5800 Hz. Shown in Fig. 3.8 is the maximum amplitude of blade response vs. frequency in this range obtained at 0.1% of mistuning standard deviation. Note that the corresponding harmonic mistuning is indeed the dominant effect, between the mean + 2 standard deviations of the response and its 95th percentile.

A similar analysis was also carried out for 1% of mistuning standard deviation and the results are presented in Fig. 3.9. Notice there that the harmonic mistuning predictions are much lower than the random mistuning ones. Clearly, this mistuning level exceeds the level at which the maximum effect of natural frequency splitting/peak separation occurs.

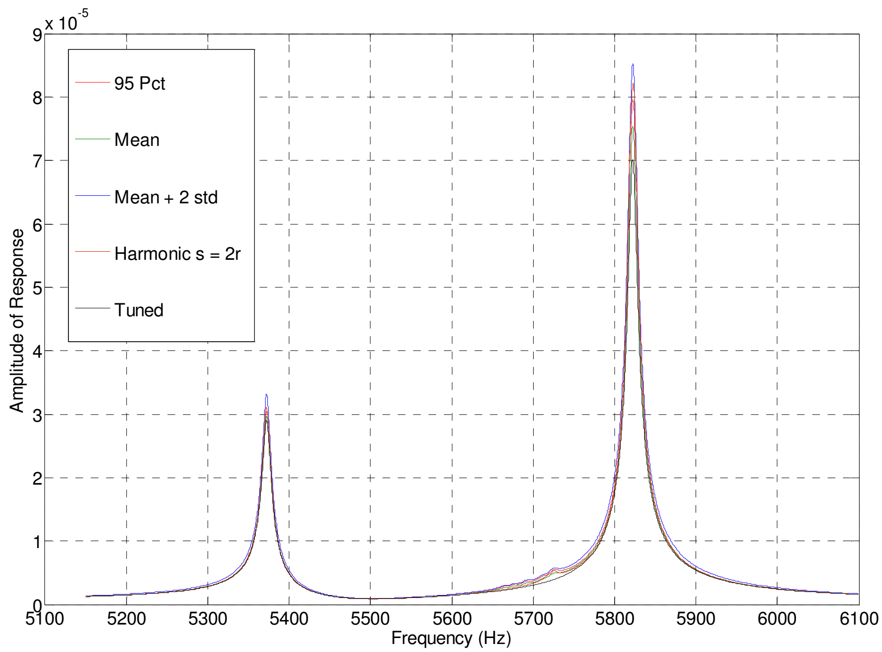

(a)

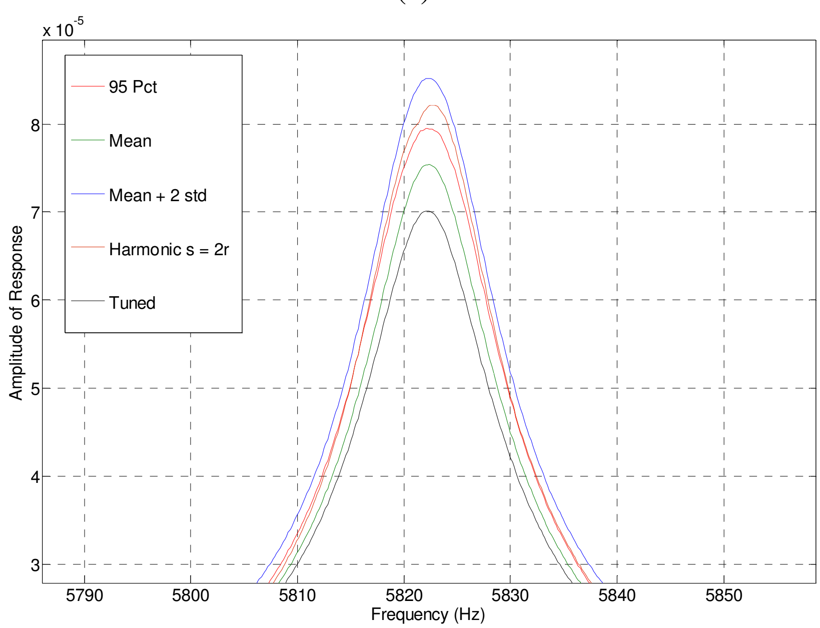

(b)

Figure 3.8.(a) Maximum Amplitude of Blade Response, Blisk Model, 1st Engine Order Excitation, 0.1% Mistuning Standard Deviation. (b) Same as (a), Zoomed.

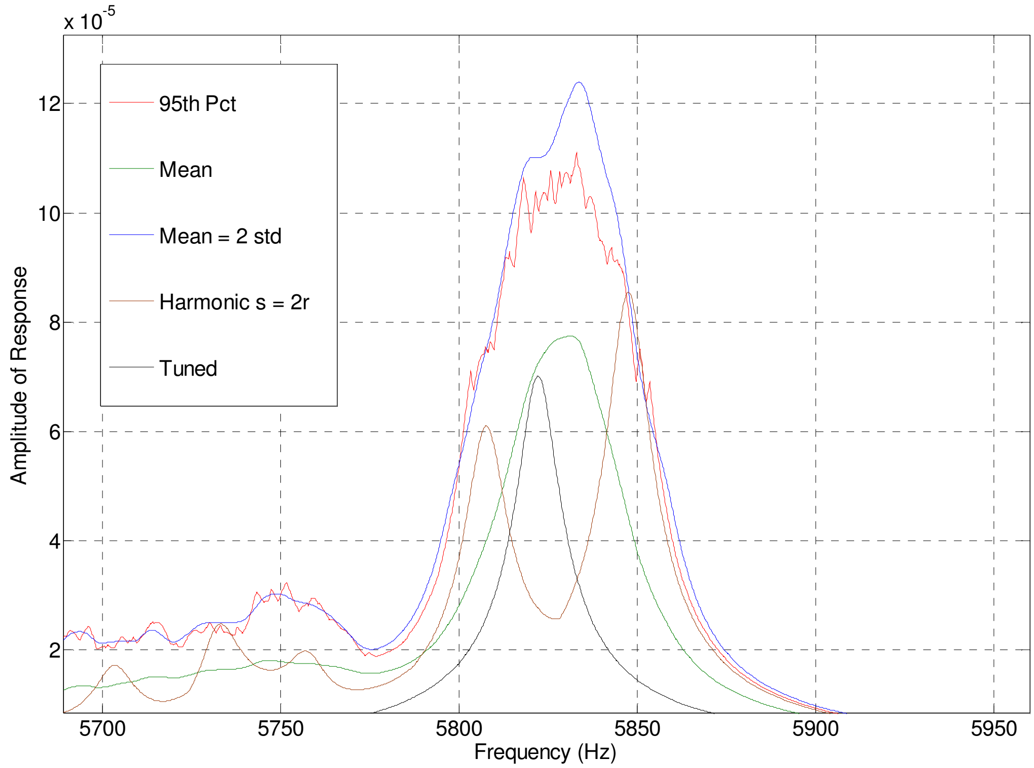

Figure 3.9. Maximum Amplitude of Blade Response (Zoomed), Blisk Model, 1st Engine Order Excitation and 1% Mistuning Standard Deviation.

In this light, additional computations were carried out (with the reduced order model for increased computational expediency) at various other levels of mistuning, random and harmonic, other harmonics of mistuning, as well as the exponential-harmonic model. Figure 3.10 presents those various computational results and note again that the exponential-harmonic model provides a good qualitative and reasonably quantitative model of random mistuning.

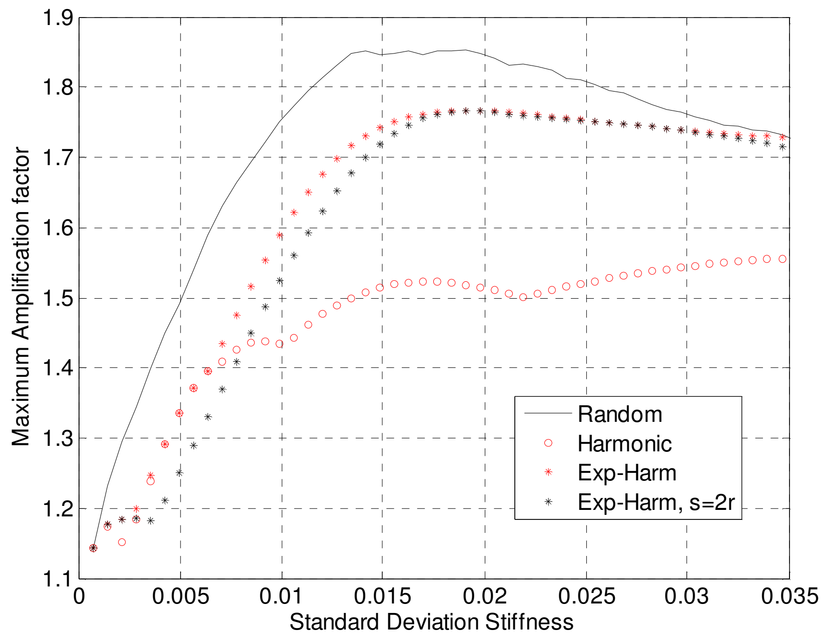

Figure 3.10. Maximum Amplification of Blade Response for Harmonic and Exponential-Harmonic Mistuning. Blisk Model of Fig. 1.2, $r = 1$.

3.4 VEERING RESONANCE OF THE BLISK FINITE ELEMENT MODEL

The previous section has focused on an isolated resonance which can reasonably be expected to be consistent with the single degree of freedom per sector mode. To assess further harmonic mistuning, a pair of resonances in a veering zone are next considered. This example was selected in the neighborhood of 7kHz at engine order 4, see Fig. 1.3. This condition is analyzed by a modal analysis of the mistuned finite element model as the reduced order model has been shown in the past not to be reliable in these conditions, as it does not correctly capture the distance between the two frequencies.

For clarification and confirmation, the mode shapes corresponding to the two modes of natural frequencies equal to 6903 Hz and 7007Hz are shown in Fig. 3.11. The blade deformations seen on these modes are similar, albeit mirror images.

The comparison between harmonic and random mistuning was again carried out as in the previous section, starting with a 0.1% change in frequency as mistuning standard deviation. Then, shown in Fig. 3.12 are the predictions obtained by both harmonic and random mistuning. Even though the two frequencies are close, the harmonic mistuning leads to an excellent match of the random results but it is unclear if there is actual interaction between the two modes. At 1% standard deviation of frequency mistuning, see Fig. 3.13, it is again seen that the harmonic mistuning significantly underpredicts the amplification factor obtained from the random mistuning analysis as in Fig. 3.9. The discussion of [6] suggests that the values of the mistuning harmonic s in the neighborhood of 2 r = 8 would likely be more representative. This is indeed the case, see Fig. 3.14 with the $s = 2\ r + 1$ (= 9) giving a substantially larger amplification, still smaller than the one obtained from random mistuning, but this increase over the $s = 2\ r$ suggests that the corresponding level of mistuning is fully in the distortion range, i.e., with amplification controlled by the distortion of the modes. A similar comparison for engine orders 1, 2, and 5, see Figs 3.15-3.17, shows a different situation. First, the harmonics $s = 2\ r$ and $s = 2\ r + 1$ give very similar peak amplitudes in all three cases. More interestingly though, the appearance of the curves is similar to the one of Fig. 3.14 with two strong peaks near 7kHz. Yet, the tuned responses corresponding to these engine orders do not show a double peak.(see Fig. 3.18) It is suggested that one of the peak (splitting as expected) originates from the excited mode while the second corresponds to another number of nodal diameters and is excited by the engine order excitation through the distortion. The possibility for this phenomenon was discussed in section 3.2.

Noteworthy in Fig. 3.13 are the very large amplification factors obtained on the two peaks, which are both approximately of the order of 2.5. Given the number of blades, 12, it is necessary to confirm the possibility to obtain such large numbers. As demonstrated in [20,21] the largest possible amplification factor can be expressed as the product of a tuned amplification factor, resulting from changes in the mean disk model, by a mistuned factor which is of the order of the Whitehead limit [22], i.e. $\left(1+\sqrt{N}\right)/2 =$ 2.23 for 12 blades. The amplification factors of 2.5 can thus be consistent only with the presence of a tuned amplification factor. To assess the existence of this term, the disk was uniformly mistuned, i.e., all blade properties were changed equally, and the changes in the peak response at the two corresponding natural frequencies in 4th engine order excitation were recorded. Shown in Fig. 3.19 are the plots of the tuned amplification factors for the left and right peaks in the veering zone as a function of the relative change in overall blade frequency. Clearly, 30% to 40% change in amplitudes can be observed with as little as 2% change in the blade alone frequencies. These large factors enable the amplification factor in random mistuning analyses to achieve the 2.5 noted earlier.

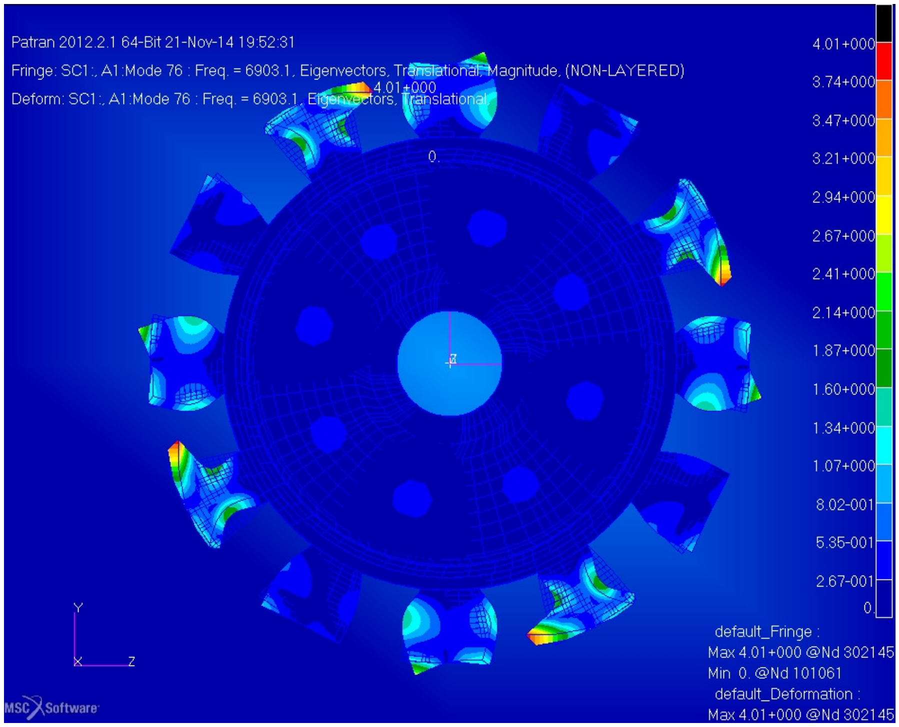

(a)

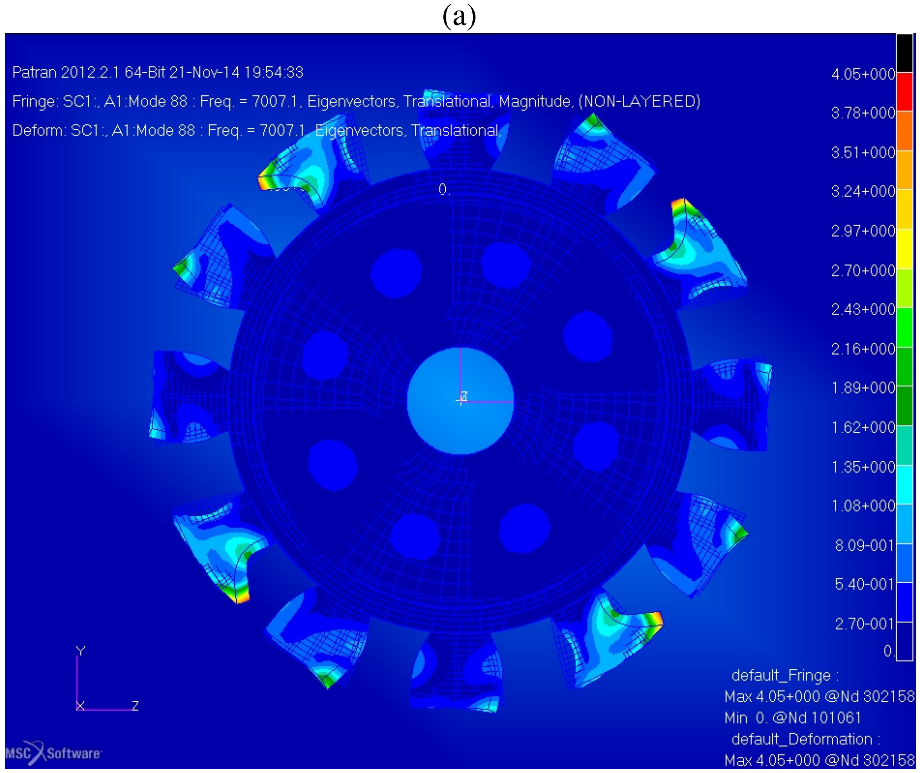

(b)

Figure 3.11. Mode Shapes of the Two Modes in Veering Near 7khz, (a) Mode of Natural Frequency 6903Hz, (b) Mode Of Natural Frequency 7007Hz.

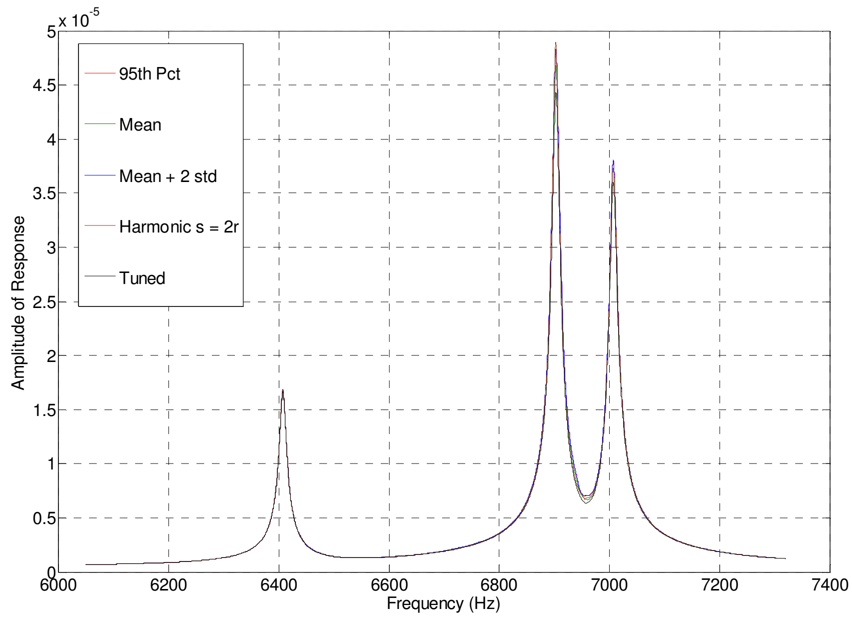

(a)

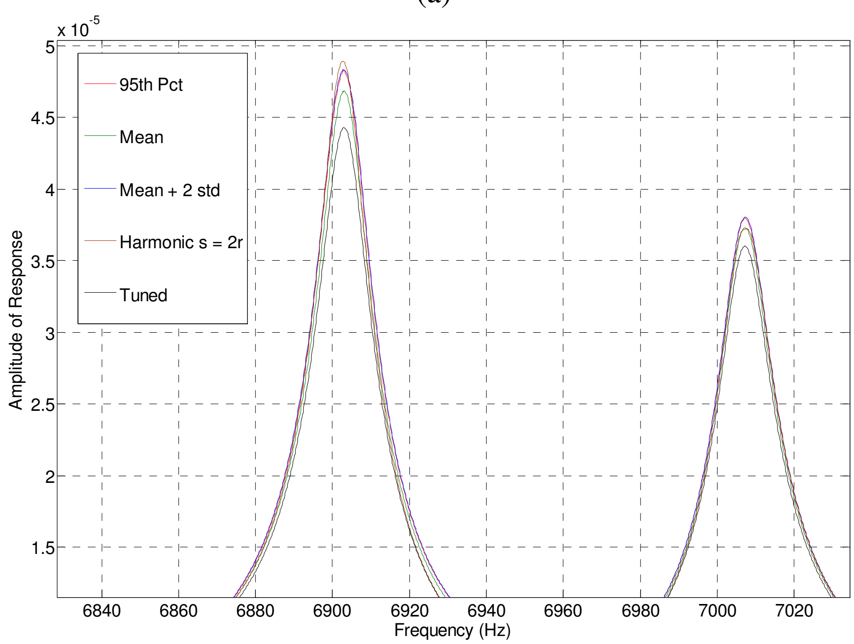

(b)

Figure 3.12. (a) Maximum Amplitude of Blade Response, Blisk Model, 4th Engine Order Excitation, 0.1% Mistuning Standard Deviation. (b) Same as (a), Zoomed.

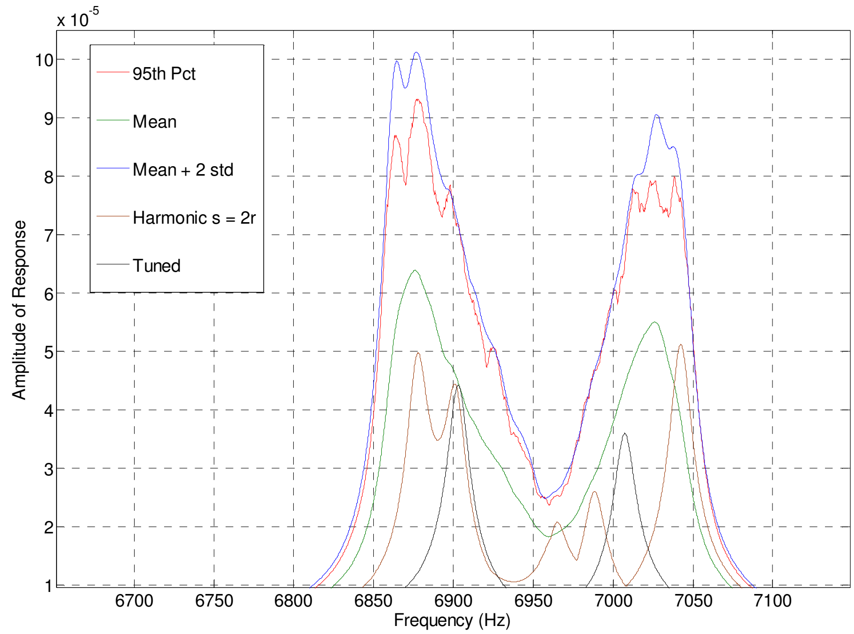

Figure 3.13.Maximum Amplitude of Blade Response (Zoomed), Blisk Model, 4th Engine Order Excitation and 1% Mistuning Standard Deviation.

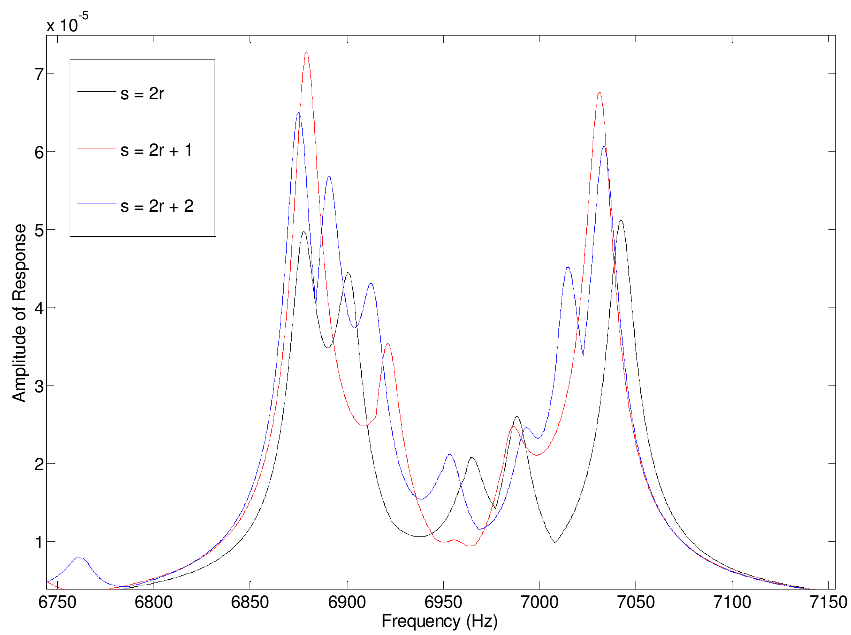

Figure 3.14. Maximum Amplitude of Blade Response (Zoomed), Blisk Model, 4th Engine Order Excitation and 1% Mistuning Standard Deviation, $s = 2\,r, 2\,r + 1$, And $2\,r + 2$ Harmonics.

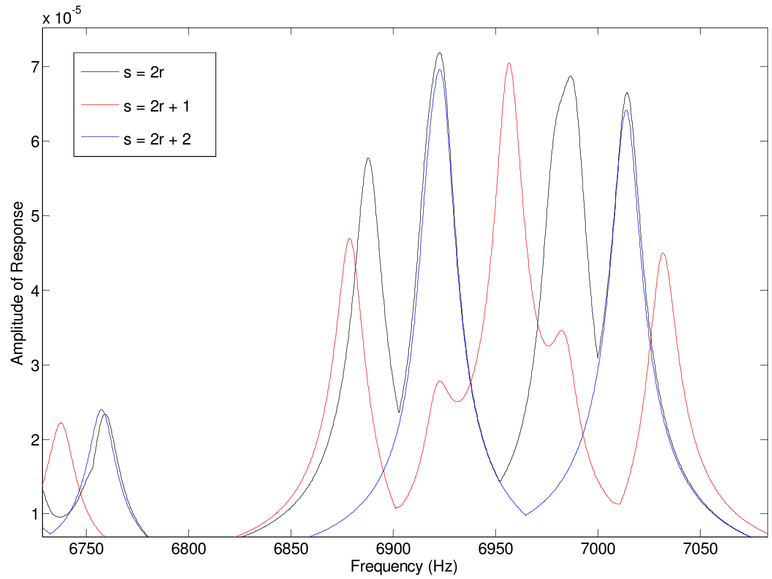

Figure 3.15. Maximum Amplitude of Blade Response (Zoomed), Blisk Model, 1st Engine Order Excitation and 1% Mistuning Standard Deviation, $s = 2\,r, 2\,r + 1$, And $2\,r + 2$ Harmonics.

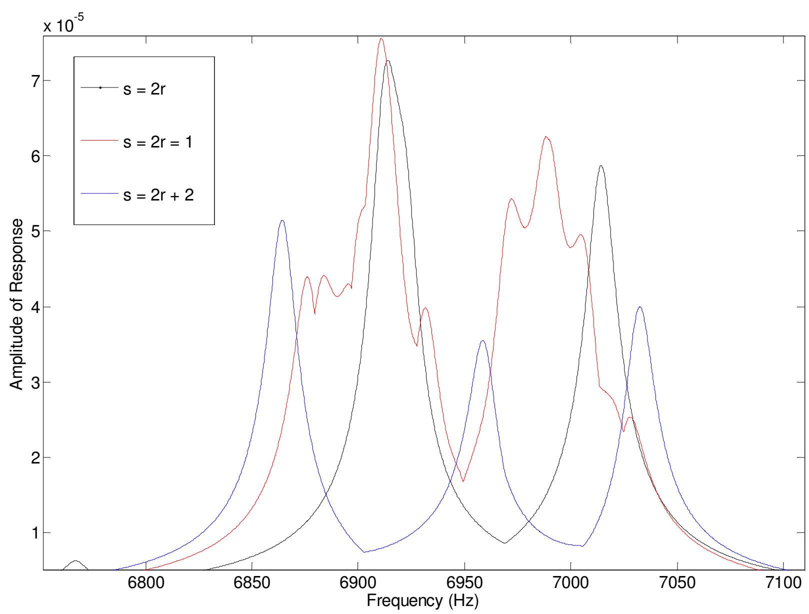

Figure 3.16. Maximum Amplitude of Blade Response (Zoomed), Blisk Model, 2nd Engine Order Excitation and 1% Mistuning Standard Deviation, $s = 2\,r, 2\,r + 1$, And $2\,r + 2$ Harmonics.

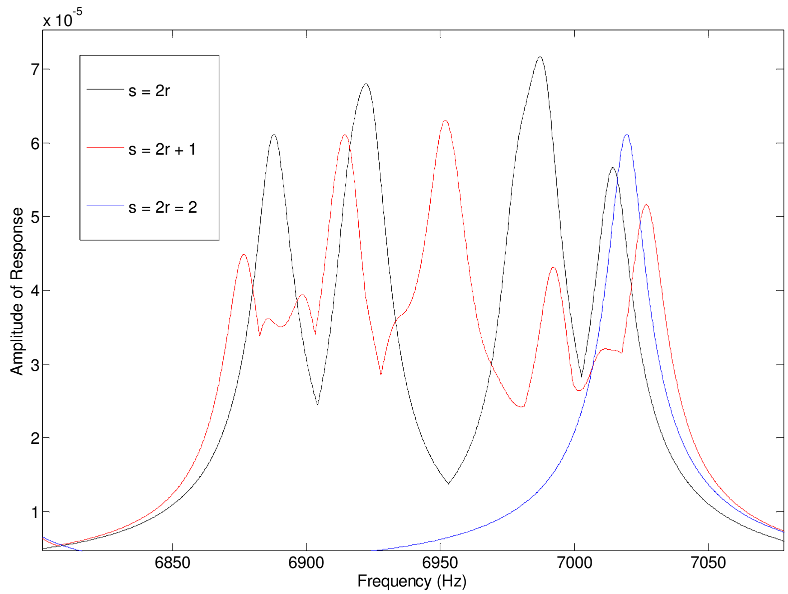

Figure 3.17. Maximum Amplitude of Blade Response (Zoomed), Blisk Model, 5th Engine Order Excitation and 1% Mistuning Standard Deviation, $s = 2\,r, 2\,r + 1$, And $2\,r + 2$ Harmonics.

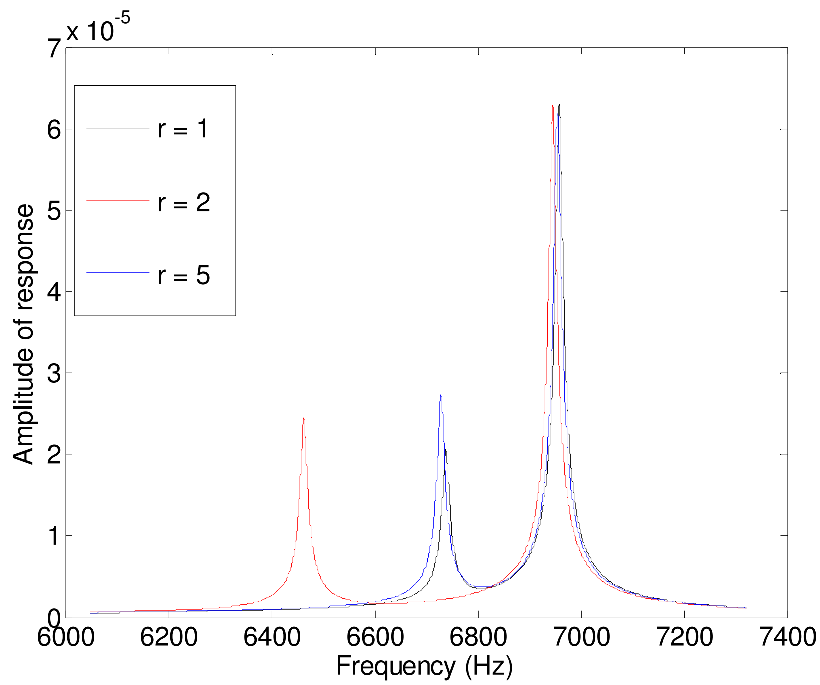

Figure 3.18. Tuned Amplitudes of Blade Response, Blisk Model, 1st, 2nd and 5th Engine Order Excitations.

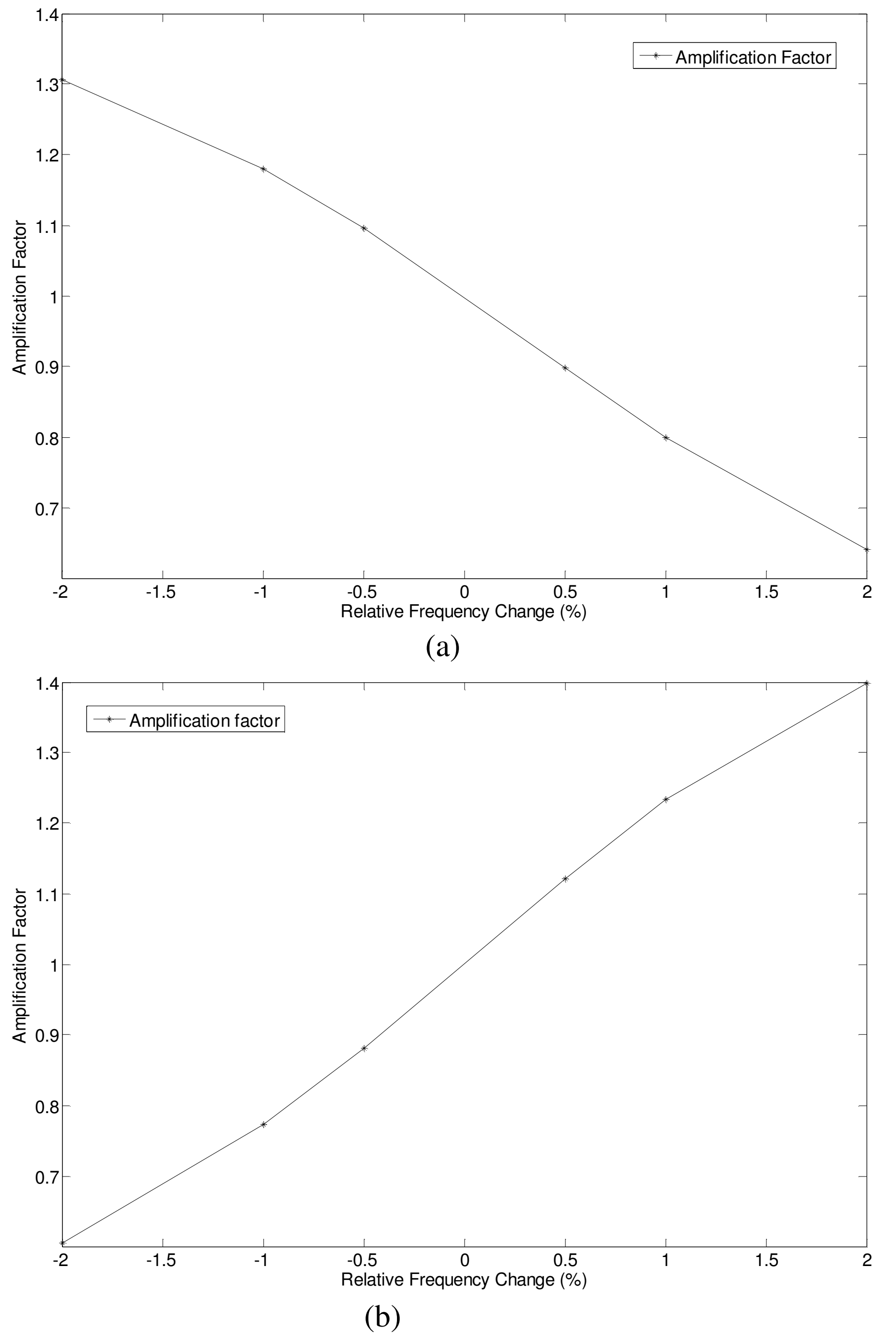

Figure 3.19. Tuned Amplification for the Left and Right Peaks of the Veering Zone.

CHAPTER 4

GEOMETRIC VS. YOUNG'S MODULUS MISTUNING

The focus of this chapter is on a preliminary assessment, on the model and resonance conditions investigated in Chapter 3, of the effects of geometric mistuning on the amplification of forced response as compared to those obtained by Young's modulus mistuning. As suggested in [9,10,12], the changes in blade geometry will be modeled as random amplitudes multiplying deterministic shape variations. The three shape variations considered here are: (i) a uniform change in blade thickness, (ii) a change in blade thickness varying linearly from blade root (where it is zero) to blade tip (where it is max), (iii) a change of blade thickness that is linearly varying from leading to trailing edge. Two sets of analyses were conducted. In the first, random variations along each of the three patterns alone were imposed and the response of the corresponding mistuned disks was determined as a function of the excitation frequency. A comparison of these results with those of Young's modulus, at equal deviation of the natural frequency provides a perspective on the effects of mode shape mistuning. A second comparison assesses these effects directly by using combinations of two different patterns to cancel out any change in natural frequency. These two analyses were conducted for both the isolated resonance and the veering conditions. Shown in Fig. 4.1 is the prediction of the maximum amplitude of blade response at the isolated resonance with the three patterns, both with random mistuning and harmonic mistuning. These figures are quite consistent with each other and with Fig. 3.9, in fact with slightly lower peak amplitudes. This analysis repeated for the veering conditions of the 4th engine order excitation leads the results of Fig. 4.2 which again are quite consistent with each other and with those obtained with

Young's modulus except that a slight increase in the magnitude of the two peaks is obtained with respect to the latter mistuning. The results would suggest that mode shape mistuning has very little effect in the isolated resonance case and only a small one in the veering case.

To confirm these expectations, combinations of 2 shape patterns were created that canceled the changes in blade alone frequencies that they created when considered alone. The three combinations 1-2, 2-3, and 3-1 were considered for both the isolated resonance and the veering case. The maximum amplitudes of blade response for these mistuned scenarios are shown on Figs 4.3 and 4.4. As expected, it is seen in Fig. 4.3 that the mode shape mistuning effects are very small, amplifications that are of the order of 3%. On the contrary, in the case of the veering, amplification of the response at the peak by approximately 25% is obtained.

It is thus tentatively concluded that mode shape mistuning effects are negligible when considering isolated resonance but provide some small, additional amplification for veering conditions.

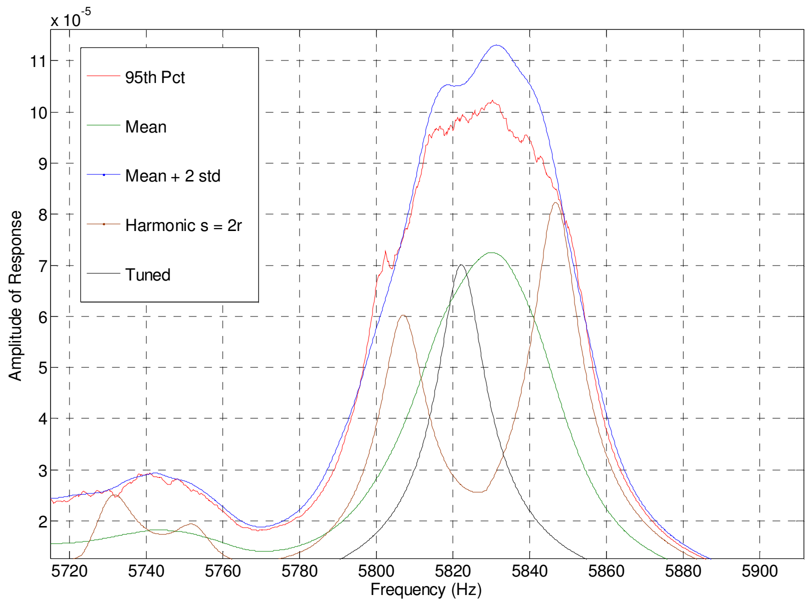
x 10^-5
95th Pct
Mean
Mean + 2 std
Harmonic s = 2r
Tuned
Amplitude of Response
Frequency (Hz)
5720
5740
5760
5780
5800
5820
5840
5860
5880
5900

(a)

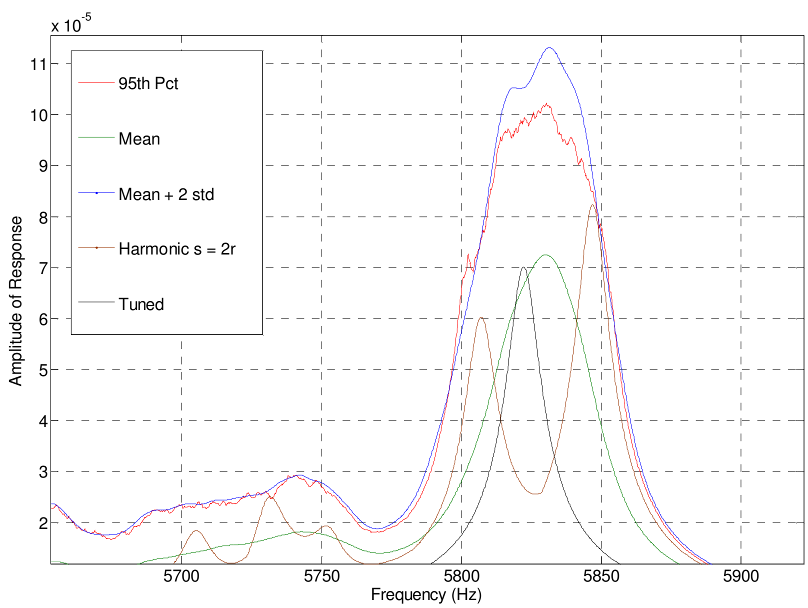
x 10^-5
95th Pct
Mean
Mean + 2 std
Harmonic s = 2r
Tuned
Amplitude of Response
Frequency (Hz)
5700
5750
5800
5850
5900

(b)

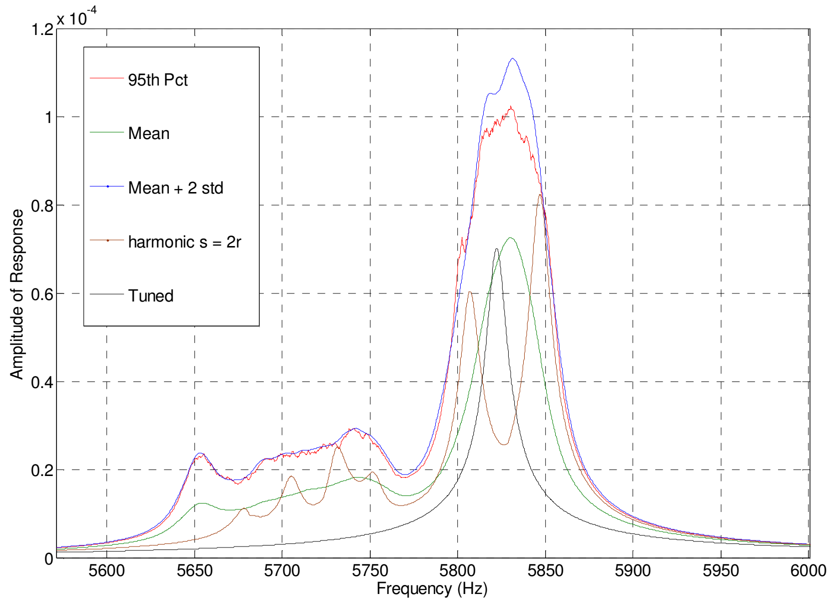

(c)

Figure 4.1. Maximum Amplitude of Blade Response, (Zoomed), Blisk Model, 1st Engine Order Excitation and 1% Mistuning Standard Deviation on Pattern (a) 1, (b) 2, (c) 3.

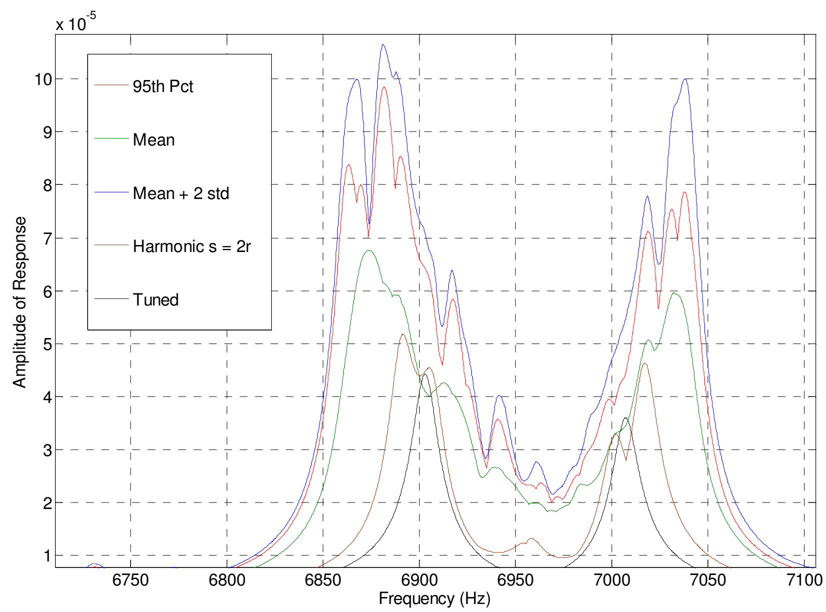

(a)

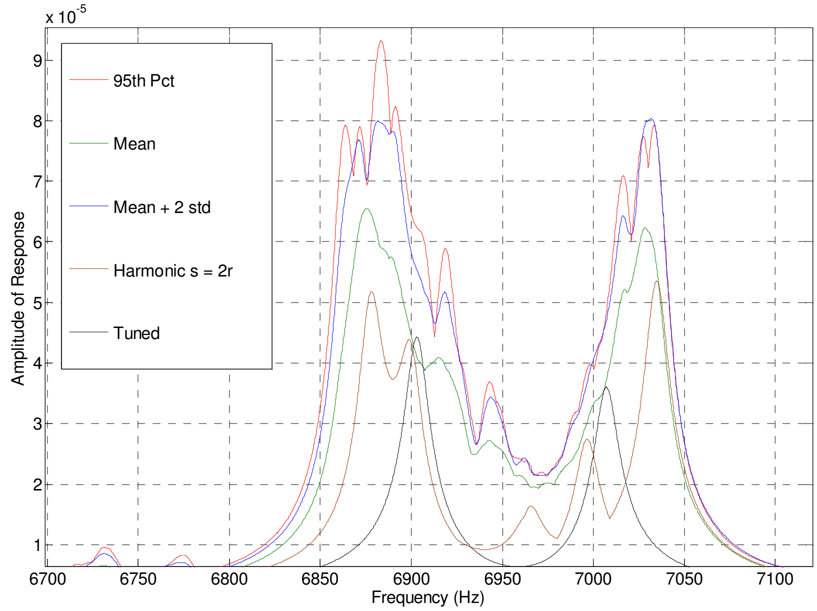

(b)

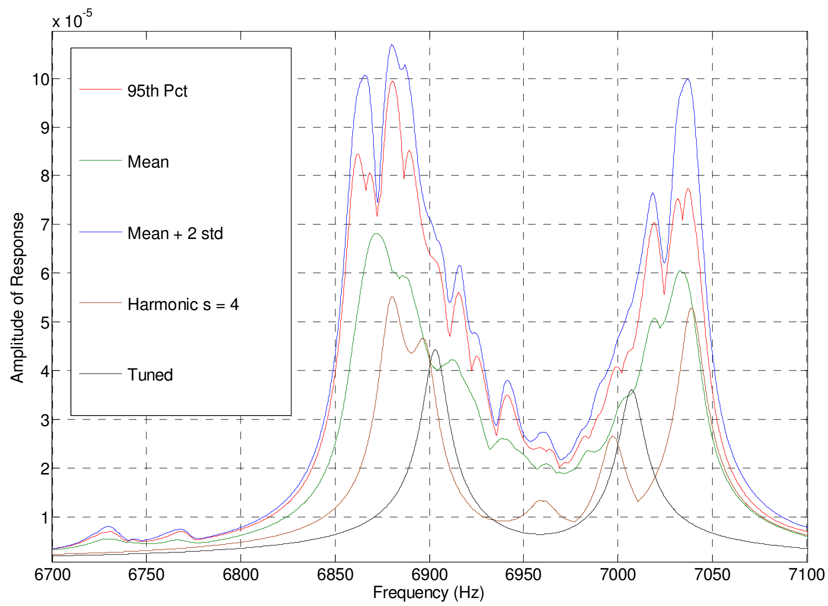

(c)

Figure 4.2. Maximum Amplitude of Blade Response, (Zoomed), Blisk Model, 4th Engine Order Excitation and 1% Mistuning Standard Deviation on Pattern (a) 1, (b) 2, (c) 3.

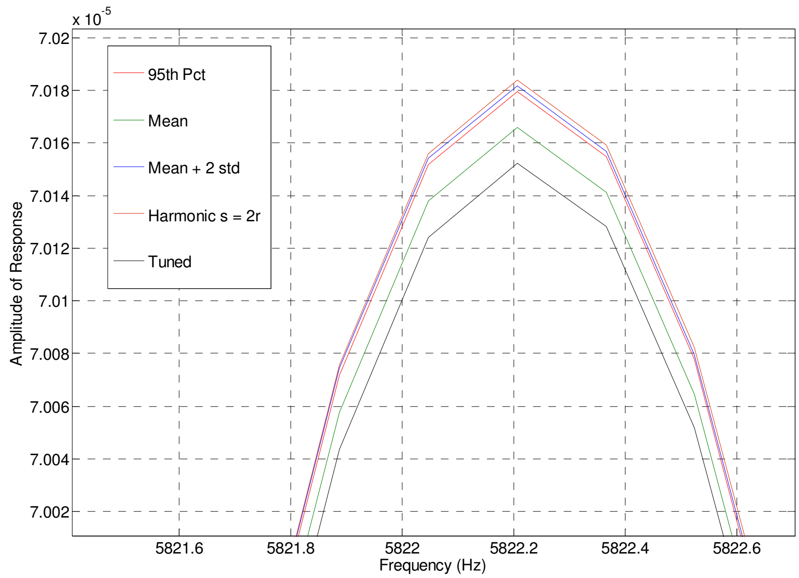
x 10^-5
7.02
7.018
7.016
7.014
7.012
7.01
7.008
7.006
7.004
7.002
95th Pct
Mean
Mean + 2 std
Harmonic s = 2r
Tuned
Amplitude of Response
5821.6
5821.8
5822
5822.2
5822.4
5822.6
Frequency (Hz)

(a)

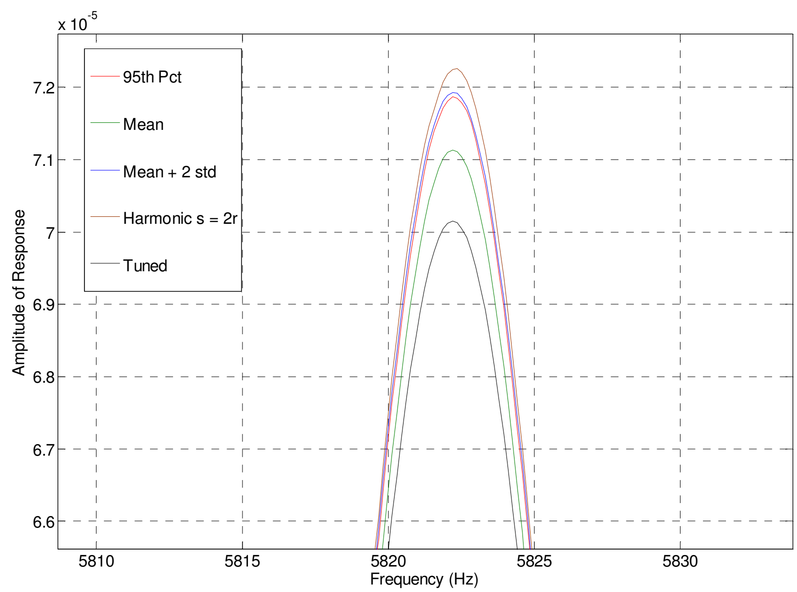
x 10^-5
7.2
7.1
7
6.9
6.8
6.7
6.6
95th Pct
Mean
Mean + 2 std
Harmonic s = 2r
Tuned
Amplitude of Response
5810
5815
5820
5825
5830
Frequency (Hz)

(b)

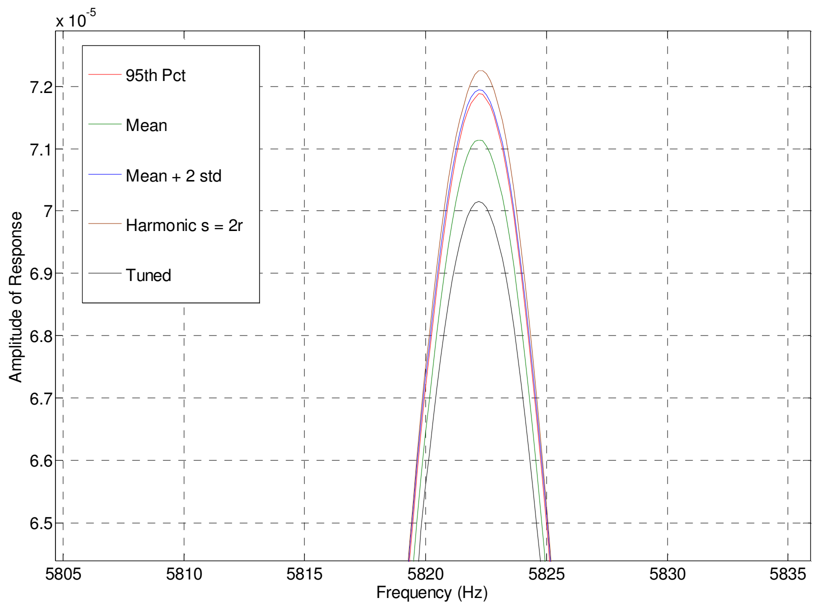

(c)

Figure 4.3. Maximum Amplitude of Blade Response, (Zoomed), Blisk Model, 1st Engine Order Excitation and Combinations of 1% Mistuning Standard Deviations on Patterns (a) 1-2, (b) 2-3, (c) 3-1.

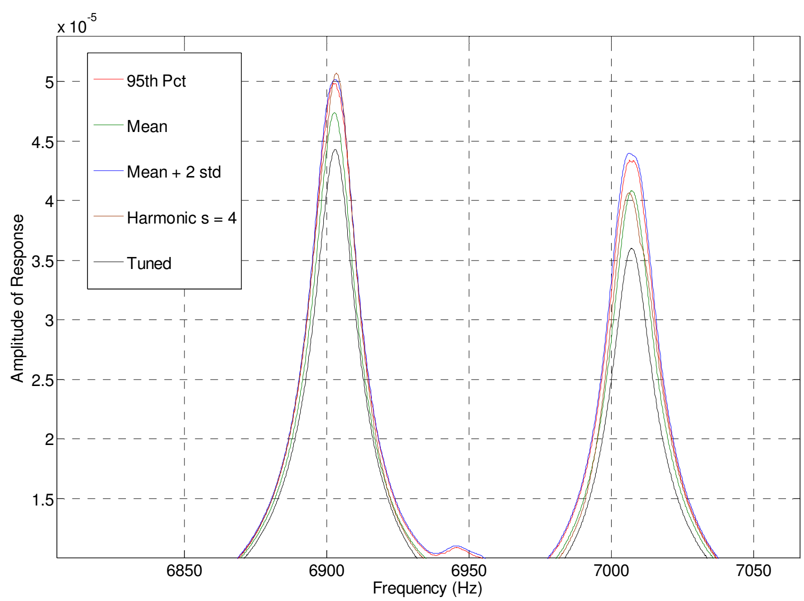

(a)

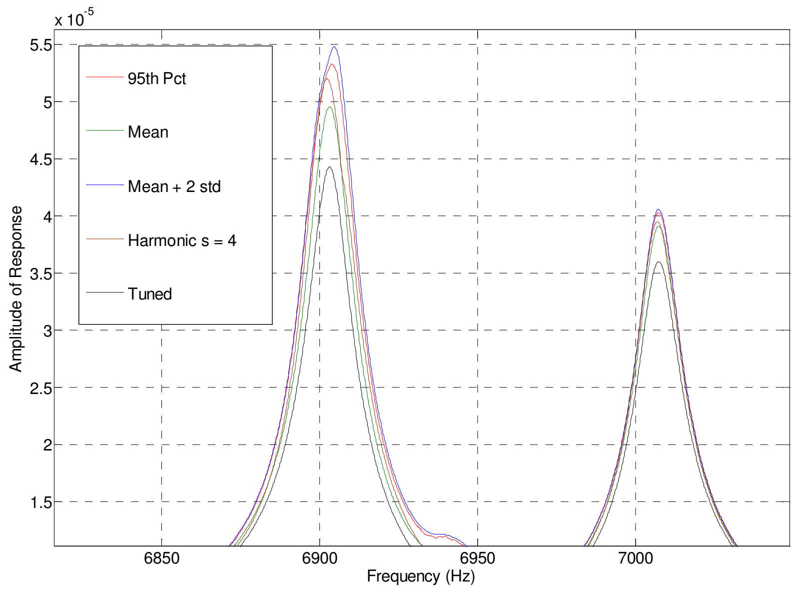

(b)

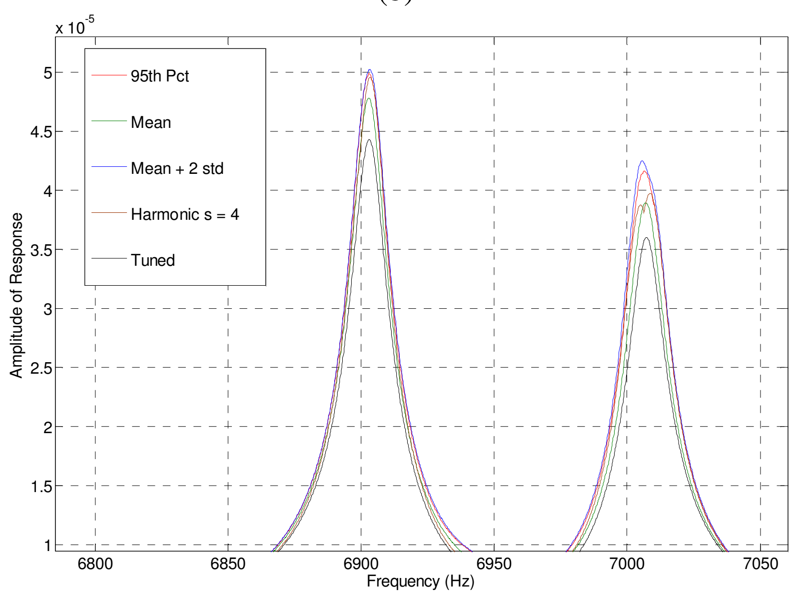

(c)

Figure 4.4. Maximum Amplitude of Blade Response, (Zoomed), Blisk Model, 4th Engine Order Excitation and Combinations of 1% Mistuning Standard Deviations on Patterns (a) 1-2, (b) 2-3, (c) 3-1.

CHAPTER 5

SUMMARY AND CONCLUSION

The focus of this thesis was first on a detailed revisit of the applicability of harmonic mistuning of rotors to provide qualitative and/or quantitative information on their response to random mistuning. The single degree of freedom per sector bladed disk model was initially revisited. As demonstrated in the earlier investigation [6], it was shown that the dominant harmonics are first $s = 2\ r$, then $s = 2\ r+1$ but it was found that the next harmonic is $s = 3\ r$, where r is the engine order of the excitation, which appears to be justified from second order perturbation arguments. The effects of the finite number of blades was also discussed, demonstrating the known but not proved low sensitivity of the $N/4$ number of nodal diameter modes to mistuning and suggesting the possible presence of $3\ r$ number of nodal diameter modes in the response if they are in the band of interest. Finally, an exponential-harmonic mistuning model was introduced that leads to a better quantitative approximation of random mistuning effects than the harmonic mistuning model. These observations were confirmed on both an isolated resonance and a veering condition of a finite element blisk model.

The final aspect of this thesis was an initial assessment of the differences in amplification of blade response induced by either Young's modulus or geometric mistuning. The physical difference between the two mistuning models is the presence in the latter of variations in blade alone mode shapes not considered in the former. The current findings were that there is extremely little difference between the two models when considering isolated resonance. However, in veering zones, a small increase in maximum blade amplitude was observed under geometric mistuning at equal change in frequency than Young's modulus mistuning. A direct analysis of the effects of mode shape mistuning was proposed that involves generating geometry variations that do not lead to any change in blade alone frequencies. This process led to amplification of blade response by about 25% in a tight veering zone.

REFERENCES

[1] Rao, J.S., Turbomachine Blade Vibration, New Age Publishing, 1991.

[2] Avalos, J., and Mignolet, M.P., "Maximum Amplification of Blade Response in Multistage Models," Proceedings of the IGTI Turbo Expo'10, Glasgow, Scotland, Jun. 14-18, 2010, ASME Paper GT-2010-23062.

[3] Bladh, R., Castanier, M. P., and Pierre, C., "Component-Mode-Based Reduced Order Modeling Techniques for Mistuned Bladed Disks–Part I: Theoretical Models," Journal of Engineering for Gas Turbines and Power, 123(1), pp. 89–99, 2001.

[4] Castanier, M.P., Ottarson, G., and Pierre, C., "A Reduced Order Modeling Technique for Mistuned Bladed Disks," Journal of Vibration and Acoustics, 119, pp. 439-447, 1997.

[5] Mignolet, M.P., Hu, W., and Jadic I., "On the Forced Response of Harmonically and Partially Mistuned Bladed Disks. Part I: Harmonic Mistuning," International Journal of Rotating Machinery, Vol. 6, No.1, 2000, pp. 29-41.

[6] Kenyon, J.A., and Griffin, J.H., "Forced Response of TurbineEngine Bladed Disks andSensitivity to Harmonic Mistuning," Journal of Engineering for Gas Turbines and Power, Vol. 125, 2003, pp. 113-120.

[7] MacBain, J.C., and Whaley, P.W., "Maximum Resonant Response of Mistuned Bladed Disks," Journal of Vibration, Acoustics, Stress, and Reliability in Design, Vol. 106, 1984, pp. 218-223.

[8] Soize, C., 2000, "A Nonparametric Model of Random Uncertainties on Reduced Matrix Model in Structural Dynamics," Probabilistic Engineering Mechanics, Vol. 15, No. 3, pp. 277-294.

[9] Sinha, A., Hall, B., Cassenti, B., and Hilbert, G., "Vibratory Parameters of Blades From Coordinate Measurement Machine Data," Journal of Turbomachinery, Vol. 130, Issue 1, Article Number 011013, 2008.

[10] Sinha, A., "Reduced-Order Model of a Bladed Disk with Geometric Mistuning," Proceedings of the IGTI Turbo Expo 07, Montreal, Canada, May 14-17, 2007, Paper GT2007-27276.

[11] Brown, J.M., and Grandhi, R.V., "Reduced-Order Model Development for Airfoil Forced Response," International Journal of Rotating Machinery, Vol. 2008, Article ID 387828, 12 pages, 2008.

[12] Bhartiya, Y., and Sinha, A., “Reduced Order Model of a Multistage Bladed Rotor with Geometric Mistuning via Modal Analyses of Finite Element Sectors,” Turbo Expo 10, Glasgow, UK, June 14-18, 2010, Paper GT2010-22725.

[13] Beck, J.A., Brown, J.M., Cross, C.J., and Slater, J.C., “Probabilistic Mistuning Assessment Using Nominal and Geomerty Bases Mistuning Methods,” Turbo Expo 12, Copenhagen, Denmark, June 11-15, 2012, Paper GT2012-68533.

[14] Wei, S. T., and Pierre, C., 1988, “Localization Phenomena in Mistuned Assemblies with Cyclic Symmetry - Part I: Free Vibrations,” Journal of Vibration, Acoustics, Stress, and Reliability in Design, 110, No. 4, pp. 429-438.

[15] Wei, S. T., and Pierre, C., 1988, “Localization Phenomena in Mistuned Assemblies with Cyclic Symmetry - Part II: Forced Vibrations,” Journal of Vibration, Acoustics, Stress, and Reliability in Design, 110, No. 4, pp. 439-449.

[16] Han, Y., and Mignolet, M.P., “A Novel Perturbation-Based Approach for the Accurate Prediction of the Forced Response of Mistuned Bladed Disks,” Presented at the IGTI Turbo Expo’07, Montreal, Canada, May 14-17, 2007, ASME Paper GT-2007-27352.

[17] Castanier, M. P., and Pierre, C., 1997, ‘‘Consideration on the Benefits of Intentional Blade Mistuning for the Forced Response of Turbomachinery Rotors,’’ Proceedings of the 1997 ASME International Mechanical Engineering Congress and Exposition, AD-55, ASME, New York, pp. 419–425.

[18] Castanier, M. P., and Pierre, C., 1998, ‘‘Investigation of the Combined Effects of Intentional and Random Mistuning on the Forced Response of Bladed Disks,’’ AIAA Paper No. 98-3720.

[19] Kiflu, B., “Analysis of Mistuned Bladed Disks by a Reduced Order Technique: Validation, Identification, and Stochastic Modeling,” M.S., Arizona State University, May 2005.

[20] Han, Y., Xiao, B., Mignolet, M.P., “Expedient Estimation of the Maximum Amplification Factor in Damped Mistuned Bladed Disks,” Journal of Turbomachinery, Accepted for Publication.

[21] Xiao, B., Rivas-Guerra, A.J., and Mignolet, M.P., “Maximum Amplification of Blade Response due to Mistuning in Multi-Degree-of-Freedom Blade Models, Journal of Turbomachinery, Accepted for Publication.

[22] Whitehead, D.S., Effect of Mistuning on the Vibration of Turbomachine Blades Induced by Wakes," Journal of Mechanical Engineering Science, Vol. 8, 1966, pp. 15-2